

**TRIBOLOGICAL CHARACTERIZATION OF
Al-Cu-Mg-B COMPOSITES SUBJECT TO
MECHANICAL WEAR**

By

Ruth G. I. Hidalgo Hernández

A thesis submitted in partial fulfillment of the requirements for the degree of

MASTER OF SCIENCE

in

MECHANICAL ENGINEERING

UNIVERSITY OF PUERTO RICO

MAYAGÜEZ CAMPUS

December, 2009

Approved by:

Paul Sundaram, Ph.D
Member, Graduate Committee

Date

Jay Banerjee, Ph.D
Member, Graduate Committee

Date

O. Marcelo Suárez, Ph.D
President, Graduate Committee

Date

Henri Radovan, Ph.D
Representative of Graduate Studies

Date

Gustavo Gutierrez, Ph.D
Chairperson of the Department

Date

Abstract of Dissertation Presented to the Graduate School
of the University of Puerto Rico in Partial Fulfillment of the
Requirements for the Degree of Master of Science

**TRIBOLOGICAL CHARACTERIZATION OF
Al-Cu-Mg-B COMPOSITES SUBJECT TO
MECHANICAL WEAR**

By

Ruth G. I. Hidalgo Hernández

December 2009

Chair: O. Marcelo Suárez

Major Department: Mechanical Engineering

The tribological properties of a series of aluminum matrix composites reinforced with AlB_2 particles developed for machinery parts intended for aerospace and automotive applications were evaluated. This thesis encompasses the microstructure characterization of those composites and the assessment of their tribological response when subject to pin-on-disk wear test. SEM and EDS analyzes permitted to identify the phases present and correlate the composite microstructure with its mechanical and tribological behavior. SEM observations also allowed identifying the wear mechanisms involved during the pin-on-disks tests against a 440 martensitic stainless steel ball. Wear coefficients were contrasted with Brinell and superficial Rockwell hardness. It was possible to establish the effect of chemical composition on the wear volume and wear coefficient for different composites compositions. This will then permit obtaining machinery parts with optimal performance, achieving high durability, high resistance and the reduction of maintenance costs.

Resumen de Disertación Presentado a Escuela Graduada
de la Universidad de Puerto Rico como requisito parcial de los
Requerimientos para el grado de Maestría en Ciencias

CARACTERIZACIÓN TRIBOLÓGICA A COMPUESTOS DE Al-Cu-Mg-B SUJETOS A DESGASTE MECÁNICO

Por

Ruth G. I. Hidalgo Hernández

Diciembre 2009

Consejero: O. Marcelo Suárez
Departamento: Ingeniería Mecánica

Las propiedades tribológicas de una serie de compuestos de matriz de aluminio reforzados con partículas de diboridos de aluminio, desarrollados para piezas de maquinarias destinadas a aplicaciones en la industria aeroespacial y automotriz, fueron evaluadas. Esta tesis abarca la caracterización de la microestructura de los compuestos y la evaluación de sus propiedades tribológicas cuando son sometidos a pruebas de de desgaste "pin-on-disk". Los análisis de microscopía electrónica de rastreo (SEM) y espectrometría de dispersión de energía permitieron identificar las fases presentes y correlacionar la microestructura del compuesto con su comportamiento mecánico y tribológico. Las observaciones en SEM también permitieron identificar los mecanismos de desgaste presentes durante las pruebas de "pin-on-disk". Los coeficientes de desgaste calculados fueron contrastados con la dureza "Brinell" y "Rockwell" superficial. Fue posible establecer el efecto de la composición química en el volumen removido y el coeficiente de desgaste de las distintas composiciones de los compuestos. Esto permitirá obtener piezas con un rendimiento óptimo, alta resistencia y la reducción de los costos de mantenimiento.

Copyright © 2009

by

Ruth G. I. Hidalgo Hernández

I dedicate this thesis:

To God, for the strength that keeps me standing.

To my parents, Yolanda Hernández and Ismael Hidalgo, whose inspiration, love and encouragement entirely supported me in every challenge that life has presented to me.

To my grandmothers, for lifting me up when this journey seemed endless.

To my sister and brothers, for their understanding and lasting love.

To Daniel Páez, my source of motivation and impulse, the partner who kept my spirit up when the muses seemed to leave me.

ACKNOWLEDGMENTS

I am heartily grateful to my advisor, Professor O. Marcelo Suárez, whose guidance, encouragement and support since my days as an undergraduate until my final steps as a graduate student enabled me to develop leadership skills and an understanding in the area of Materials Science. My gratitude is also to the members of my committee, Professors Jayanta Banerjee and Paul Sundaram, for their assistance in perfecting this thesis.

This research would not have been successful without the assistance and collaboration of Nayomi Plaza, Carlos Osorio, Alexis Torres, Alberto Callejo, Daniel Suárez, and Roberto Rivera, Mechanical and Chemical Engineering undergraduate students, Hermes Calderón and Humberto Melgarejo, graduate students and Prof. Kumar Sridharan from the University of Wisconsin-Madison, and Alexander Pulliza, Mechanical Engineering Department technician.

I would like express my thanks to the Puerto Rico Louis Stroke Alliance for Minority Participation: Bridge to Doctorate Program (NSF Grant N HRD-0601843) for the fellowship that helped support me during my graduate education. This material is based upon work supported by the National Science Foundation under Grants No. DMR-0351449 (PREM Program), HRD-0833112 (CREST Program) and the US Department of Energy, Savannah River through Grant No. DE-FG09-07SR22571. Hardness instrumentation used was acquired with the support from the US Department of Defense through contract No. W911NF-07-1-0611 (HBCU/MI ISP Program). KB Alloys (Reading, PA) is kindly acknowledged for the donation of the master alloys employed in the present research.

Special thanks are also obliged to all my laboratory partners and friends, especially Laura Lara and Aracelis Rosado for always being there. Lastly, I offer my regards and blessings to all of those who supported me in any respect during the completion of my studies.

TABLE OF CONTENTS

		<u>page</u>
ABSTRACT ENGLISH	ii
ABSTRACT SPANISH	iii
ACKNOWLEDGMENTS	vi
LIST OF TABLES	x
LIST OF FIGURES	xi
LIST OF ABBREVIATIONS	xiv
LIST OF SYMBOLS	xv
1	INTRODUCTION	1
1.1	Literature Review	2
1.2	Objectives	6
1.2.1	Specific Objectives	7
1.3	Thesis Structure	7
2	THEORETICAL BACKGROUND	8
2.1	Basics of Metal Matrix Composites	8
2.1.1	MMCs Advantages	10
2.1.2	Mechanism of Reinforcements	10
2.2	Mechanical Properties of Aluminum Matrix Composites	12
2.2.1	Aluminum-Boron System	13
2.2.2	Alloying with Cu	14
2.2.3	Alloying with Mg	15
2.3	Surface Wear	17
2.3.1	Classification of Wear Mechanism	18
2.3.2	Wear Scar and Debris	23
2.3.3	Wear of MMC	24
2.3.4	Wear Equation	25
2.3.5	Testing Methods	27
3	METHODOLOGY	30
3.1	Materials	31
3.2	Preparation of the Composite	32

3.3	Metallographic Preparation	33
3.4	Materials Characterization	34
	3.4.1 Microstructure	34
	3.4.2 Hardness	35
	3.4.3 Pin-on-disk Test	36
4	COMPOSITES CHARACTERIZATION RESULTS AND DISCUSSIONS	39
4.1	Microstructure Analysis	39
	4.1.1 Optical Microscopy	39
	4.1.2 Scanning Electron Microscopy (SEM)	41
4.2	Hardness Study	44
	4.2.1 Superficial Rockwell Hardness	44
	4.2.2 Brinell Hardness	46
4.3	Tribological Testing Analysis	47
	4.3.1 Pin-on-disk Test	47
	4.3.2 Wear Characteristics	47
	4.3.3 Characterization of Wear	53
4.4	Discussion	69
5	CONCLUSIONS	74

LIST OF TABLES

<u>Table</u>		<u>page</u>
2-1	Classification of types of wear based on mechanisms	19
2-2	Characterization of types of wear based on wear scars and wear debris	24
2-3	ASTM standard practices for wear testing	28
3-1	Chemical composition in weight percent of the Al-B-Cu-Mg composites studied	31
4-1	Average values of the depth and width of wear track for each sample measured with the optical profilometer	50
4-2	Removal Rate (mm^3/s) as function of boron percentage in the samples	52
4-3	Wear Mechanisms as function of boron percentage in the samples . . .	72

LIST OF FIGURES

<u>Figure</u>	<u>page</u>
2-1 Different types of metal matrix composites	9
2-2 Al-B phase diagram	13
2-3 Al-Cu phase diagram	15
2-4 Al-Mg phase diagram	16
2-5 Models of interaction between a corrosive agent and a worn surface . .	21
2-6 Delamination wear mechanism	23
3-1 Experimental methodology flow chart	30
3-2 Particle volume fraction as function of wt.%B	32
3-3 Mold, graphite crucible and furnace used for composite manufacturing	34
3-4 LECO LR-50 Rockwell hardness testing system	35
3-5 TH130 Brinell hardness tester	36
3-6 a) Pin-on-disk test apparatus constructed at UPRM, b) Components of pin-on-disk test apparatus	38
3-7 Schematic view of pin-on-disk measuring system applied	38
4-1 Microstructure of Al-2.5%Cu-1%Mg-2%B composite	40
4-2 AlB ₂ cluster shown at higher magnification in Al-2.5%Cu-3%Mg-3%B composite	40
4-3 Optical micrographs showing the AlB ₂ distribution while boron levels increases from 0 wt.% to 4 wt.% a)Al-2.5%Cu-1%Mg-0%B, b)Al- 2.5%Cu-1%Mg-1%B, c)Al-2.5%Cu-1%Mg-2%B, d)Al-2.5%Cu-1%Mg- 3%B, e)Al-2.5%Cu-1%Mg-4%B	41
4-4 a)SEM image of Al-2.5%Cu-1%Mg-2%B, b)Global EDS spectrum of the worn surface detected in Al-2.5%Cu-1%Mg-2%B composites . .	42
4-5 EDS mapping analysis of Cu on the surface of Al-2.5%Cu-1%Mg-2%B composite	43

4-6	Al-2.5%Cu-1%Mg-2%B sample a)SEM micrograph b)EDS elemental map of magnesium	43
4-7	Superficial Rockwell hardness (HRS 15T)	45
4-8	Brinell hardness (HB)	46
4-9	3-D optical Zygo New View 6300 profilometer system	49
4-10	3-D profile image of Al-2.5%Cu-3%Mg-2%B sample	49
4-11	Wear volume as function of boron percentage in the samples	51
4-12	Values of wear coefficient of the tested samples versus the AlB ₂ particles	53
4-13	Optical micrographs of wear tracks of a)Al-2.5%Cu-3%Mg-2%B composite, b)Al-2.5%Cu-3%Mg-0%B composite	55
4-14	3-D Optical profiler of wear track a)Al-2.5%Cu-1%Mg-1%B, b)Al-2.5%Cu-1%Mg-4%B composite	55
4-15	Wear track width as function of AlB ₂ particles	56
4-16	SEM micrographs of wear track illustrating grooves, ploughs and debris for identical testing conditions a)Al-2.5%Cu-1%Mg-0%B composite, b)Al-2.5%Cu-1%Mg-3%B composite, c)Al-2.5%Cu-1%Mg-4%B composite	57
4-17	SEM micrographs of pin-on-disk track on Al-2.5%Cu-1%Mg-0%B composite	58
4-18	SEM micrograph showing the dark areas analyzed by EDS in Al-2.5%Cu-1%Mg-4%B composite	59
4-19	EDS spectrum analysis of wear track: a)Al-2.5%Cu-1%Mg-0%B composites, b)Al-2.5%Cu-1%Mg-3%B composite	60
4-20	SEM micrographs and Oxygen elemental maps of: a)Al-2.5%Cu-3%Mg-0%B, b)Al-2.5%Cu-3%Mg-3%B	61
4-21	SEM image of Figure 4-17 showing the oxides in the worn surface	61
4-22	SEM micrographs showing grooves due to abrasive wear: a)Al-2.5%Cu-0%Mg-1%B composite and b)Al-2.5%Cu-0%Mg-3%B composite	62
4-23	Ploughing effects observed using SEM for: a)Al-2.5%Cu-3%Mg-0%B composite b)Al-2.5%Cu-0%Mg-1%B composite	63
4-24	SEM micrographs showing evidence of delamination wear damage (arrows): a)Al-2.5%Cu-0%Mg-1%B composite, b)Al-2.5%Cu-1%Mg-3%B composite	65

4-25 a)(arrows) Apparent delamination of Al-2.5%Cu-0%Mg-1%B composite and b)(arrows) prominent surface crack on Al-2.5%Cu-0%Mg-1%B composite	66
4-26 a)Wear sheet formation as observed using secondary electron imaging of Al-2.5%Cu-3%Mg-0%B composite b)rectangle in (a) at higher magnification	67
4-27 a)Layers of debris attached to the surface as a result of delamination wear in Al-2.5%Cu-3%Mg-3%B composite b)rectangle in (a) at higher magnification	68
4-28 Schematic illustration of particles reinforcements protecting the matrix from wear	72
4-29 SEM images of: (a) and (b) show evidence of resistance to plastic flow of Al-2.5%Cu-0%Mg-1%B composite c)(b) at higher magnification	73

LIST OF ABBREVIATIONS

MMCs	Metal Matrix Composites
AMCs	Aluminum Matrix Composites
FGM	Functionally Graded Material
DIN	Deutsches Institut fr Normung eV (German Institute for Standardization)
ASTM	American Society for Testing and Materials
RR	Removal Rate
HT	Heat Treatment
HRS	Superficial Rockwell Hardness
HB	Brinell Hardness
SEM	Scanning Electron Microscopy
EDS	Energy Dispersive Spectroscopy

LIST OF SYMBOLS

Al	Aluminum
Cu	Copper
Mg	Magnesium
AlB ₂	Aluminum Diborides
SiC	Silicon Carbide
Al ₂ O ₃	Aluminum Oxide
SiO ₂	Silica
wt%	Weight Percent
V	Wear Volume
d	Sliding Distance
F	Applied Force
k	Wear Coefficient
v_r	Relative Velocity
t	Time
dV	Amount of Material Removal
mm ³	Cubic Millimeters
N	Newtons
m	Meters
M	Required Amount of Alloy
w_f	Weight Percent in Composite
w_o	Weight Percent in Master Alloy

CHAPTER 1

INTRODUCTION

In the practice of designing, an important step to take into consideration is the minimization of wear produced in a process of any mechanical system, especially for certain aerospace and automotive applications. In recent years metal- matrix composites (MMCs) have been widely used in industries because of their excellent mechanical properties and wear resistance. In particular, a series of high strength, lightweight aluminum matrix composites (AMCs) reinforced with AlB_2 particles was developed[1] for aerospace applications. It was demonstrated that these composites can be further strengthened by convenient precipitation hardening treatments similarly to Al-Cu alloys. The high hardness attained in these Al/ AlB_2 composites made them particularly attractive for high wear applications where low density is also necessary[2], for instance in aerospace machinery parts as those required for lunar exploration. The present research is meant to establish the effect of chemical composition on the results of wear volume and wear coefficient for different Al/ AlB_2 composites, measured after subject to pin-on-disk testing.

Wear can be defined as a process which results in the loss of material from a surface by means of some mechanical or chemical actions. The environments and mechanical actions which affect wear include sliding loads, impact loads, speed, and temperature, among others. The present research addresses the wear properties of aluminum matrix composites containing copper and magnesium with reinforcing AlB_2 dispersoids, at different levels of boron. Additionally, the wear mechanisms involved in the process and the composites hardness are also studied. Optimal manufacturing conditions are determined based on several parameters: chemical composition, wear response and hardness. The pin-on-disk wear tests as well as hardness experiments will simulate the composite response to wear in service.

1.1 Literature Review

Metal matrix composites have different, and often improved or more desirable, properties as compared to their monolithic metal counterparts [3]. Taking that into consideration, depending on the particular metal and the phase used as reinforcement in a composite material, the characteristics should improve with respect to strength, stiffness, contact wear resistance and elevated temperature strength in comparison with the monolithic metal. Moreover, depending on the reinforcement phase present in the composite, the metal matrix materials may

be less expensive to manufacture. Significant applications of MMCs are included in aerospace applications, automotive components, machine parts, and electronic packaging.

On the other hand, aluminum is poor in wear resistance and is more vulnerable to seizure than steel. Nevertheless, novel lightweight aluminum matrix composites of high strength and reinforced with AlB_2 particles are currently proposed as sliding materials due to their low density and high corrosion resistance with excellent mechanical properties and low manufacturing cost [4]. Their enhanced properties include good ductility, corrosion resistance, high thermal and electrical conductivities and high damping capacity; in addition these composites can be thermally treated (precipitation hardenable materials) [5].

It is well known that boron reacts with liquid aluminum producing AlB_2 . This diboride acts as reinforcement and increases the strength of the composite, which has low production costs [1]. Additionally, copper increases matrix strength, does not react with the AlB_2 and makes the Al-matrix hardenable, improving the mechanical properties of the composite [6]. The effect of copper and magnesium on the wear behavior and microstructure has already been studied[7–13]. However, thus far there has been no attempt to analyze the concurrent addition of both elements to the composite. One can theorize that the main

impact will occur on the matrix microstructure and hardness. Moreover, the beneficial yet individual effect of copper and magnesium in the strengthening of the Al/AlB₂ composites has already been established. While copper can harden the composite matrix through precipitation of metastable compounds [14], magnesium promotes solid solution strengthening [15].

To understand the wear behavior of different MMC materials, wear tests are often carried out and have been reported. The principal tribological parameters that control the friction and wear performance of reinforced aluminum composites can be classified into two categories: one is mechanical and physical factors, and the other one is the material factor [16]. Reviewing the mechanical and physical factors (such as sliding velocity and normal load), Alpas et al. studied the effect of particle reinforced MMCs under different applied load and eventually identified three different wear regimes [17]. At low load regime, the particles support the applied load (regime I). At regime II, wear rates of MMCs and Al alloy were similar. At high load and the transition to severe wear (regime III), the surface temperatures exceed a critical value resulting in severe wear.

Many researchers have analyzed the material factors (such as volume fraction, type and size of reinforcement) and concluded that the volume fraction of reinforcement has the strongest effect on the wear

resistance [17–19]. Miyajima and Iwai investigated the effects of the reinforcement type such as whiskers, fibers and particles, on the wear process and the wear rates, concluding that particle reinforcements are most beneficial for improving the wear resistance of MMCs [20].

Melgarejo et al. studied functionally graded (FGM) Al-Mg-B composites, and showed pin-on-disk wear data, which revealed qualitatively and quantitatively the material wear response [21]. In addition it was found that Mg had a beneficial effect on the formation of the composition gradient, which favors a larger concentration of hard diborides on and near the surface of the material.

In the present study, the resulting matrix of the composite will be a ternary Al-Cu-Mg alloy since that matrix is mostly depleted of boron, which is only present in the diboride particles. Evidently, even at low temperatures (327°C), there still exists a significant solubility of Cu and Mg in the Al solid solution [22], which will contribute greatly to the overall wear resistance of the Al-B-Cu-Mg composites. Before the actual production of a specific part, it should be noted that the basic material can be further optimized to increase the wear resistance. Since matrix behavior is the main focus of this research, the principal variable will be the response to wear measured on that matrix as a function of the chemical composition.

Dry sliding wear tests were conducted using a pin-on-disk tester with Al-B-Cu-Mg composites as disks and a 440 martensitic stainless steel ball as a pin. Low contact load and small sliding velocity were selected to offset excessive heating in the samples. Wear mechanisms, weight loss and wear rate allows studying the wear characteristics of the test specimens. However, some studies indicate that specific wear coefficient is a better parameter to use [23]. This is because the wear coefficient takes taken into account not only the wear rate, the applied load, but also the hardness of the wear pin or counterface which affects the wear rate significantly [23]. As a result, AMC reinforced with AlB_2 were used in the present research to simulate the composite response in service.

1.2 Objectives

The main objective for this research is to fabricate a lightweight AMC exhibiting high wear resistance, which would make the material an appealing alternative for machinery parts intended for aerospace and automotive applications. The research investigates an aluminum matrix composite containing copper and magnesium and reinforced with AlB_2 particles. The project includes the full characterization of tribological properties of these composite materials when subject to

pin-on-disk test. The target consists of establishing the effect of chemical composition on the wear volume removed and wear coefficient for different composites compositions. This would then permit obtaining machinery parts with optimal performance, achieving high durability, high resistance and the reduction of maintenance costs.

1.2.1 Specific Objectives

- Study the hardening effect in the Al-Cu-Mg matrix reinforced with different loadings (percentage) of AlB_2 particles.
- Calculate the wear coefficient and wear volume using standard tribological tests.
- Identify the resulting wear mechanisms in these materials.

1.3 Thesis Structure

Chapter 2 summarizes the theory of surface wear, as well as the main characteristics of the AMCs studied and the systems involved in the research. In Chapter 3, the methodology for the fabrication and metallographic preparation of the Al-B-Cu-Mg composites, as well as the characterization techniques are described. Chapter 4 presents the results obtained and the experimental data analysis for the research. Finally the conclusions are provided in Chapter 5.

CHAPTER 2

THEORETICAL BACKGROUND

2.1 Basics of Metal Matrix Composites

Most mechanical systems encounter friction and wear. For this reason, automotive and aerospace industries are using metal matrix composites (MMCs) due to their higher wear resistance. MMCs, like all composites, consist of at least two chemically and physically distinct phases, suitably distributed to provide properties not obtainable with either of the individual phases[24]. MMCs are materials that have a metal or alloy as the matrix phase, which is a monolithic alloy and the reinforcement or dispersoid which consists of high performance carbon, metallic, or ceramic additions and may be in the forms of particulates, fibers, or whiskers (Figure 2-1 [25]). These composites are developed by casting, powder metallurgy and in situ from conventional production and processing of metals. The term metal matrix composites is frequently associated with the term light metal matrix composites. MMCs are a class of materials with potential for a wide variety of structural and thermal management applications.

These innovative materials open up unlimited possibilities for modern material science and development; the characteristics of MMCs can be designed into the material, custom-made, dependent on the application[25]. MMCs are capable of providing higher temperature operating limits than their base metal counterparts, and they can be tailored to give improved strength, stiffness, thermal conductivity, abrasion resistance, creep resistance, or dimensional stability[26].

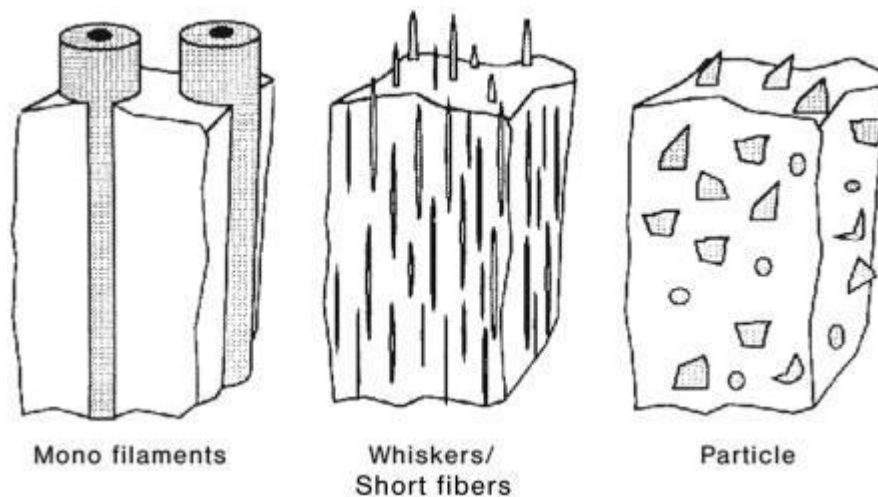


Figure 2–1: Different types of metal matrix composites

The principles of integrating a high performance second phase with a conventional engineering material and develop an improved material to obtain features not accessible from the individual constituents have been studied by many researchers. From these characteristics, metal matrix composites fulfill all the desired conceptions of the designer. This material group becomes interesting for use as constructional and functional materials, if the property profile of conventional materials

does not reach the increased standards of specific demands[25].

2.1.1 MMCs Advantages

After considerable efforts in the scientific area to produce MMCs with light metal matrices, it is well known that the successful application of these materials are found more often in areas of engineering in the automotive and aerospace industries. MMCs offer the following advantages to these areas[27]:

- Better fatigue and wear resistance
- Better elevated temperature properties
- Higher strength
- Lower creep rate
- Lower coefficients of thermal expansion

2.1.2 Mechanism of Reinforcements

Reinforcements in MMC release the option of applications in areas where weight reduction and optimization of properties are a main concern. These reinforcement materials can be produced in the form of continuous fibers or filaments, short fibers, whiskers, or particles. Examples of continuous fibers are graphite, silicon carbide (SiC), boron, and aluminum oxide (Al_2O_3), while discontinuous reinforcements mostly are of SiC in whiskers form and particle types of SiC or Al_2O_3 . For

metal reinforcement ceramic particles are often used, due to their high strength and elastic modulus with high temperature capability[24]. Recent studies have focused mainly on discontinuously reinforced (particle or whisker) aluminum matrix composites because of lower production costs[28–31].

Role of Reinforcements

The role of the reinforcement differs with its type in structural MMCs. The function of the reinforcement is to strengthen and harden the composite by reducing or eliminating matrix deformation by mechanical restraint[32]. MMCs reinforced with particle and whisker have the characteristic to be the major load bearing component. In MMCs reinforced with continuous fibers, these are the principal load bearing parts and the metallic matrix works as bonding to the reinforcements to provide integrity to the composite. Discontinuous fiber reinforced MMCs can be seen as an intermediate situation between the particulate and continuous fiber MMCs. Normally the reinforcements are used to enhance the strength, stiffness and behavior at high temperature of MMCs. When combined with a metallic matrix of higher density, the reinforcement also serves to reduce the density of the composite, thus enhancing properties such as strength[26].

2.2 Mechanical Properties of Aluminum Matrix Composites

Aluminum metal matrix composites (AMCs) are a group of composite materials, which have emerged as a promising class of materials with desirable properties including low density, high stiffness, high strength, increased fatigue resistance and higher dimensional stability at elevated temperatures. The demand for light weight, low-cost and energy efficient materials has led to the development of cast Al alloy matrix composites including hard ceramic dispersoids[33]. These Al-based MMCs have the advantage of possessing good mechanical and tribological properties[34]. The combination of light weight, environmental resistance, and useful mechanical properties has made aluminum alloys the materials of choice as a matrix metal. The melting point of aluminum is high enough to satisfy many application requirements, yet low enough to render composites fabrication reasonably convenient[26]. For most of AMCs the bonding strength is associated with a slight interfacial reaction resulting from the affinity between the alloying elements and the reinforcement[35]. AMCs have seen successful applications in the aerospace, automotive, electronic packaging, and recreational product markets.

2.2.1 Aluminum-Boron System

Aluminum's electrical conductivity can be improved by the addition of boron to settle the residual amounts of chromium, titanium, vanadium, and zirconium. Boron reacts with aluminum producing AlB_2 and AlB_{12} and with those impurities to form heavier diborides that can be removed. In particular, AlB_{12} is a high temperature phase, whereas AlB_2 is stable at room temperature when the boron content is less than 44.5 wt.%, according to the Al-B phase diagram in Figure 2-2[36]. This diboride acts as reinforcement and increases the strength

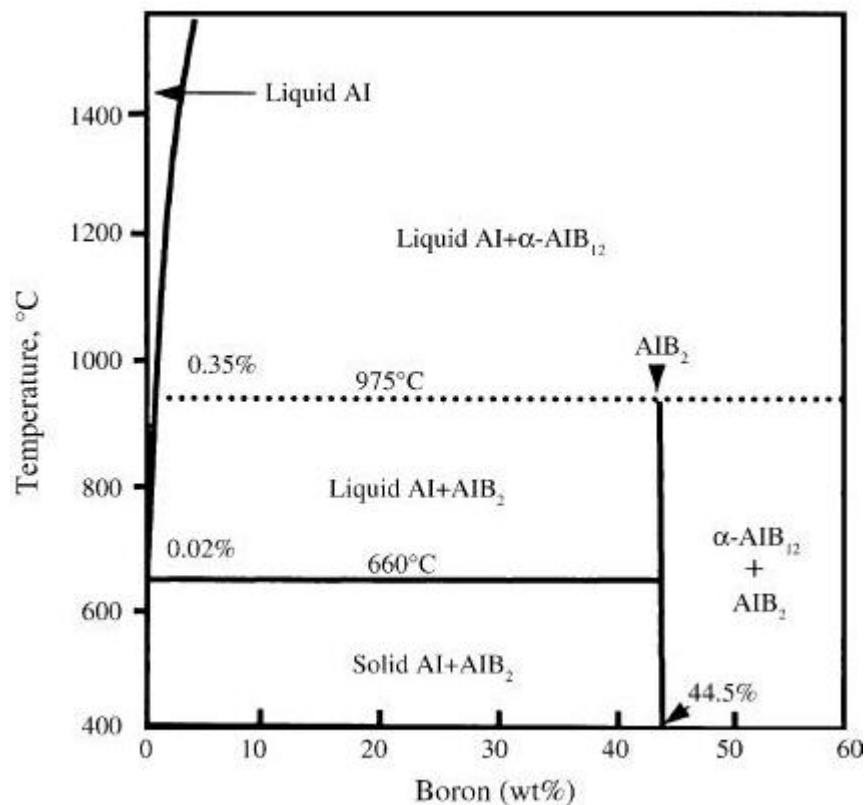


Figure 2–2: Al-B phase diagram

of the composite, which has low production costs[1]. Aluminum boron

master alloys provide a convenient source of borides for alloying purposes. Borides have also been accredited as an effective grain refiner in aluminum alloys that can provide additional strengthening to the matrix.

2.2.2 Alloying with Cu

Copper is one of the most important alloying elements for aluminum, because of its significant solubility in α -Al and strengthening effect[37]. Cu dissolves into the liquid Al phase instead of reacting with the borides. Upon normal cooling conditions, copper forms a solid solution with the Al matrix and tends to form Al_2Cu [5] according to Figure 2-3[38]. In addition copper can increase Al strength by precipitation hardening. Since Cu has a low solubility in α -Al at room temperature, a Al-Cu alloy quenched from solid solution state retains copper atoms in solid solution and becomes metastable. Therefore, given an opportunity copper atoms will tend to leave the solid solution and form a second solid phase (precipitates). This can occur even at room temperature, so that hardness will change as a function of time, a phenomenon known as natural age hardening[38].

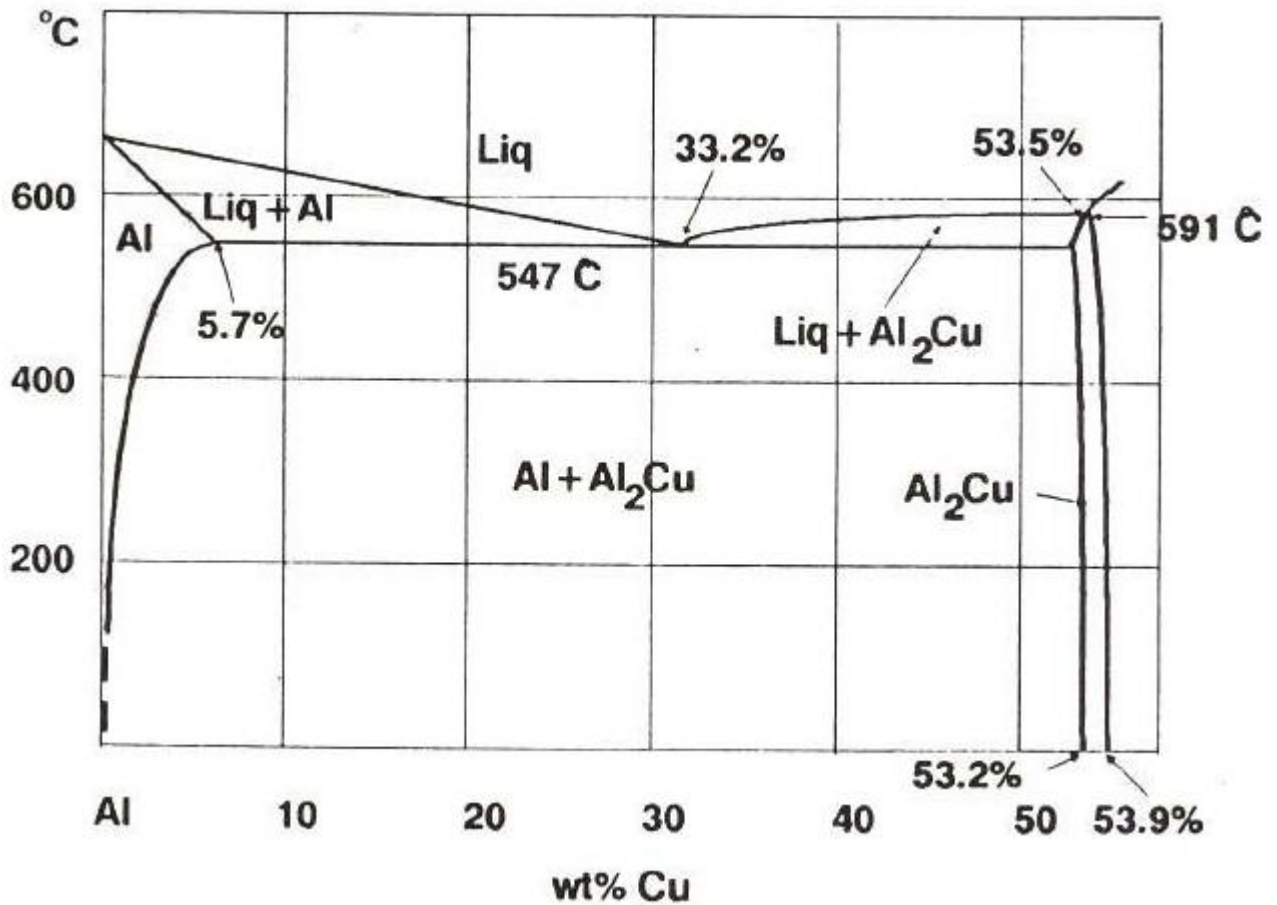


Figure 2-3: Al-Cu phase diagram

2.2.3 Alloying with Mg

Al-Mg alloys are well suited for applications where low density, ease of fabrication, structural durability, and most notably, resistance to corrosion is a necessity. Aluminum-magnesium alloys offered moderate to high strength and toughness. These alloys have excellent weldability, machinability, and an attractive appearance in applications requiring a bright surface finish, outstanding response to chemical finishing and corrosion resistance[39]. For every 1 wt% Mg in solid

solution the aluminum density decreases linearly by approximately 0.5 % [6]. According to the Al-Mg equilibrium phase diagram, Al-Mg alloys with a magnesium concentration on the order of or below 5% are solid solutions, with substitutional Mg atoms (Figure 2-4 [40]). Although at room temperature a thermodynamic driving force for the formation of the intermetallic phase Al_3Mg_2 exists, the kinetics of its formation are very slow [41]. In practical terms, this causes a metastable solution to exist at room temperature without a strong tendency to form precipitates of a second phase.

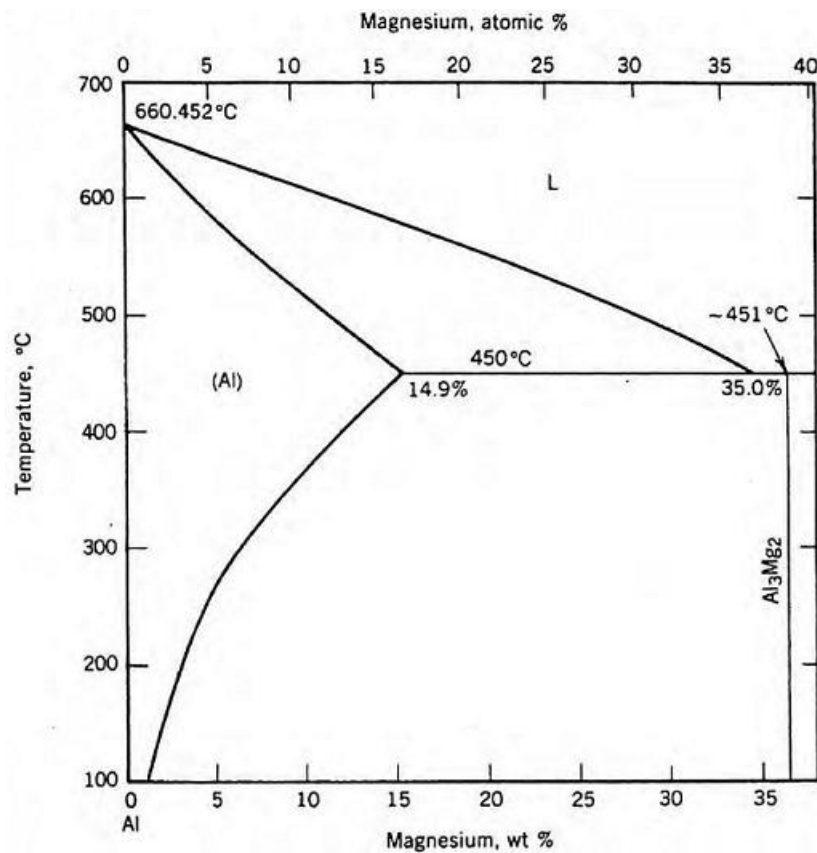


Figure 2-4: Al-Mg phase diagram

2.3 Surface Wear

Wear is defined as the surface and/or sub-surface damage or removal of material from one or both of two contacting solid surfaces in a sliding, rolling, or impact motion relative to one another, involving a progressive loss of material[42]. Wear of materials is controlled by the material characteristics and working factors such as applied pressure, sliding speed, environment and the type of sliding interaction. In general the term wear is emphasized on loss of material, but it should be pointed out that damage due to material displacement on a given body, with no net change in weight or volume, also constitutes wear[43]. According to the standard DIN 50320, wear is not an intrinsic property of the material but a system response[44].

In recent years, the development of wear resistance systems in industry has become a crucial subject from both engineering and economic standpoints. Consequently, studies on prevention and solution of wear problems in industry have increased their focus on performance improvement. Surface wear is one of the most common problems in industry, leading to recurrent replacement of components.

2.3.1 Classification of Wear Mechanism

Recently, important progresses in investigations has been made in the understanding of wear mechanisms, leading to enhance the efficiency and performance of many engineering systems. Wear mechanisms may acquire several appearances depending on the surface topography, the contact conditions and the environment. Commonly, wear mechanisms can be classified as two main types, mechanical and chemical. Mechanical wear involves processes which may be associated with friction, abrasion, erosion and fatigue. Chemical wear take place mainly in surface attack by reactive compounds followed by rubbing or detachment of reaction products by mechanical action[45]. Different types of wear may take place individually, sequentially or simultaneously, but all the wear mechanisms concentrate on a common characteristic: surface damage (Table 2-1 [44]). The common mechanical wear mechanisms include:

- Abrasive wear
- Adhesive wear
- Corrosive wear
 - Oxidative wear
- Fatigue wear
 - Delamination wear

Table 2–1: Classification of types of wear based on mechanisms

Wear Type	Mechanism
Adhesion	Formation of interfacial adhesions "weld" junctions by the action of molecular forces
Abrasion	Grooving by scratching and ploughing action, microcutting process
Fatigue	Cracking at the surface due to stresses or strains varying in magnitude or direction

Abrasive Wear

Abrasive wear occurs when asperities of a rough, hard surface or hard particles slide on a softer surface and damage the interface by plastic deformation or fracture[42]. Generally, a material is seriously abraded or scratched only by a particle harder than itself. When ductile materials with high fracture toughness are present the wear by hard asperities or hard particles results in the plastic flow of the softer material. Examples for this case are most of the metallic and ceramic surfaces, in which the sliding process demonstrates evidence of plastic flow. Abrasion can be categorized as: a) low stress process, when the abrasive material remains fairly intact; b) high stress process, when the abrasive material is crushed; and c) ploughing, when a relative large abrasive phase will cut the material. Some of the mechanisms involved in the abrasive wear are [46]:

- **Ploughing:** the material is displaced from a groove to the sides. This does not result in any real material loss, as the abraded material remain attached to the damaged surface.

- Cutting: the most severe form of abrasive wear, where abraded chips are removed.
- Microcracking: small cracks are formed due to high stresses.

Adhesive Wear

Adhesive wear occurs when one material is in sliding motion over another with surface interaction and welding at localized contact areas. Adhesion (or bonding) occurs on the asperity contacts at the interface; these contacts are sheared by sliding, which may result in detachment of a fragment from one surface and attachment to the other surface[42]. The adhesion joints are small locations of impurities that would be irrelevant in a large specimen but in practice may be sufficient to allow shearing through the harder material. In theory, this type of wear does not remove material but simply transfers it between wearing surfaces[47]. Adhesive wear may occur among metallic materials, ceramics or polymers, or combinations. It is dependent on adhesion between the materials; that in turn depends on surface films like oxides or lubricants, as well as the mutual affinity of one material for another.

Corrosive Wear

Corrosive wear is defined as the degradation of materials in which both corrosion and wear mechanisms are involved[43]. Corrosive wear is present when material loss occurs through electrochemical attack at

the surface assisted by mechanical wear. However, corrosive wear is not the summation of the loss of material caused due to the mechanical wear and corrosion. Sometimes corrosion accelerates the wear process and vice versa; therefore, the loss of material is definitely larger than when they are summed up independently[48]. The corrosive wear takes place in a corrosive environment. Schematic models of corrosive wear are shown in Figure 2-5[49].

Oxidative Wear. The most common form of corrosion is due to a reaction between the metal and oxygen, generally called oxidative wear. In this form of wear metallic oxides mixed with the worn metal form debris layers of mixed metal and oxide[49]. Corrosion products, usually oxides, have shear strengths different from those of wearing surface metals from which they were formed. The oxides tend to flake away, resulting in the pitting of wearing surfaces[47].

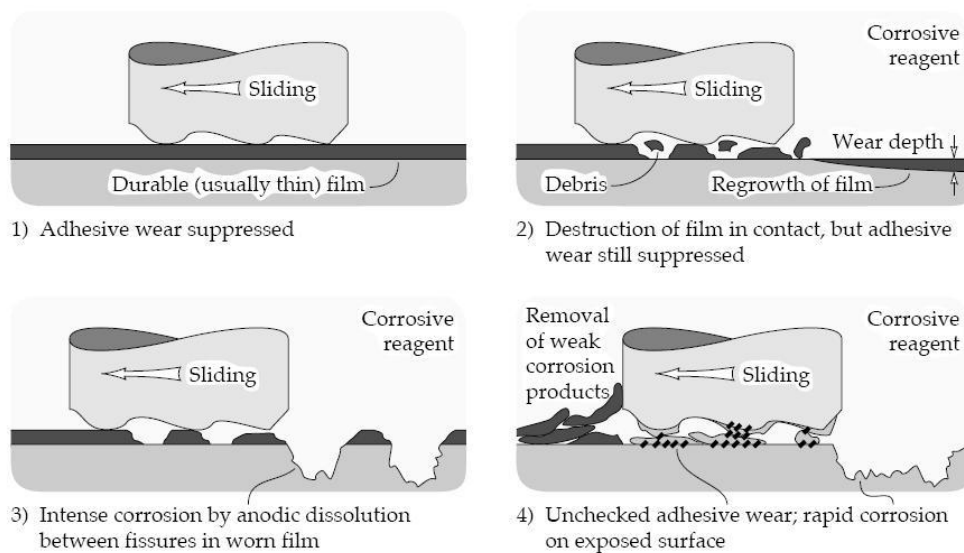


Figure 2-5: Models of interaction between a corrosive agent and a worn surface

Fatigue Wear

Fatigue wear is defined as the resultant wear when surface failure is generated by fatigue after repeated friction cycles[50]. Fatigue wear can be produced in both plastic and elastic contacts. The material removal in this type of wear is governed by deformation and fracture in the contact region during repeated sliding or rolling conditions, where fracture modes are fatigue, brittle, or ductile fracture. Such deformation and fracture are generated by mechanically induced strains and stresses. The repeated loading and unloading cycles to which the materials are exposed may induce the formation of surface or subsurface cracks, which eventually will result in the breakup of the surface with the formation of large fragments leaving large pits in the surface[42].

Delamination Wear. The delamination wear is the loss of metal due to the plastic flow of the material in conjunction with constant sliding (Figure 2-6). This mechanism is part of fatigue wear mechanism in which subsurface cracks propagate parallel to the surface and shear producing long and thin wear sheets or flakes, giving rise to plate-like debris. The cracks are initiated at voids and vacancies developed below the surface by dislocation pile-ups[51]. The delamination theory was introduced in 1972 by Nam P. Suh, to explain wear of metals. The theory affirmed the frequent observation of wear debris in the form of flakes[52].

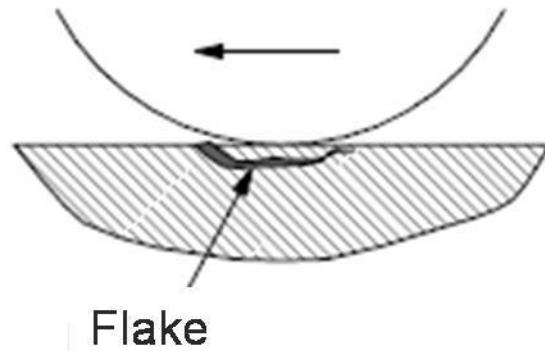


Figure 2-6: Delamination wear mechanism

2.3.2 Wear Scar and Debris

The repetitive action of wear generates the formation of small shallow damage points, representing loss of material, known as wear scar. The cumulative wear damage scar and wear debris can be utilized to recognize the type of wear (Table 2-2). In practice, more than one type of wear process may lead to multiple surface damage resulting in compound wear scars. However, in such case, the predominant wear process sometimes leaves a characteristic impression so that identification is possible. Studying the wear scar and debris is an important part of wear failure analysis. Closer examination, requiring high resolution and greater field of depth, can be done with scanning electron microscope (SEM). The use of energy-dispersive analytical techniques along with SEM can provide information on nature and composition of wear debris[44]. Wear debris comes in many sizes and shapes. Study of wear debris morphology and chemistry can provide evidence of work

conditions and the wear mechanism involved[50].

Table 2–2: Characterization of types of wear based on wear scars and wear debris

Type of Wear	Wear particle/debris	Wear scar
Adhesion	Flakes Splinters	Sliding tongue wedge
Abrasion	Particles, Flat Splinters	Grooves or furrows running parallel to surface; Discontinuous if hard phase present in wear track; Comet tails in low stress abrasion
Thermal	Oxides Particles or flakes	Scale, partly or fully covering the surface; Pits/cavities

2.3.3 Wear of MMC

A large amount of engineering materials have been employed for applications in which wear resistance is a key requirement, such as MMCs. The reason for the success of this type of material in tribological applications can be explained, in a simplified form, by stating that the toughness of the matrix together with the hardness of the reinforcement particles enables optimal wear resistance[53].

The MMCs possess excellent combination of mechanical and physical properties like high stiffness, strength and hardness in addition to lightweight and high abrasion resistance, as compared to the monolithic alloys. As mentioned before, these composites have found many applications in the aerospace and automotive industry. The competitive advantages of MMCs over other metallic systems as tribomaterials include their unique ability to[54]:

- Develop a composite to meet specific engineering strength and stiffness requirements.
- Improve the fatigue, creep, and stress-rupture properties of the metals.

2.3.4 Wear Equation

In order to study this behavior, predictive equations should take into account factors, such as material, component geometries and appropriate operating conditions. There has been controversy concerning wear theory for over a century and it is improbable that a single governing equation will be established to cover all eventualities. Therefore, the general form of the wear equation is based on the relationship developed by Archard[55]. It has been demonstrated that for a wide range of conditions, both adhesive and abrasive, the wear volume (V) is directly proportional to the sliding distance (d) and the applied normal force (F) and are related as follows:

$$V = kFd \quad (2.1)$$

where k is termed the dimensional wear coefficient, conventionally in units of $\text{mm}^3/\text{N m}$. An equation of this form was proposed by Archard in relation to adhesive wear and extended by Rabinowicz to

more general cases of abrasive wear and is often known as the Archard equation[56].

The dimensionless wear coefficient k is essential and important. It provides a valuable resource for comparing the rigorousness of wear processes in different systems. This dimensional coefficient correspond to the volume of material removed by wear (in mm^3), per unit of distance slid (in meters), per unit normal load on the contact (in Newtons). The measure of wear provided by k is particularly helpful for comparing wear rates in different classes of material[57].

Archard equation can be modified to Preston equation to calculate the material removal rate (RR)[58–61]. According to Preston equation:

$$\frac{dV}{dt} = kFv_r$$

$$RR = kFv_r \tag{2.2}$$

the relative velocity (v_r) between the sphere pin and the specimen surface, the applied load F , and the time t are the main parameters determining the amount of material removal dV .

2.3.5 Testing Methods

Many different experimental arrangements have been used to study wear. Investigations related to wear usually examine the mechanisms by which wear occurs, or simulate practical applications and provide useful design data on wear rates and coefficients of friction. To understand the wear behavior of different MMCs, wear tests are often carried out with suitable wear testing techniques. ASTM's wear standards are used to provide the appropriate procedures for wear tests and determine the amount of material removal during a specified test period under well defined conditions (Table 2-3).

A significant amount of test methods have been designed for the evaluation of wear and friction properties obtained by test equipments, frequently known as tribometers. The tests presented here are the most frequently used for different applications and represent appealing recent developments in the field of tribotesting[50].

Pin-on-disk Test

A pin specimen is held and pressed tightly against a flat circular disk with a specified load applied by an arm or lever. During the test, either the pin or the disk rotates, and the sliding path forms a circular scar on the disk surface. The amount of wear is determined by weighing or measuring the dimensions before and after the test. Linear dimensional changes can be measured by electronic distance gaging or

stylus profiling. Linear measurements are converted to wear volume by using suitable geometric relations. This test is perhaps the most commonly used during the development of materials for tribological applications[44].

Table 2–3: ASTM standard practices for wear testing

Standard	Wear Test Methods
G 59	Conducting Potentiodynamic Polarization Resistance Measurements
G 65	Measuring Abrasion Using the Dry Sand/Rubber Wheel Apparatus
G 73	Liquid Impingement Erosion Testing
G 75	Determination of Slurry Abrasivity Abrasity and Slurry Abrasion Respose of Materials
G 76	Conducting Erosion Tests by Solid Particle Impingement Using Gas Jets
G 98	Galling Resistance of Materials
G 99	Wear Testing with a Pin-on-Disk Apparatus
G 102	Calculation of Corrosion Rates and Related Information from Electrochemical Measurements
G 105	Conducting Wet Sand/Rubber Wheel Abrasion Tests

Pin-on-Flat(Recicropating) Test

A flat plate moves relative to a stationary pin in reciprocating motion. In some cases, the plate is stationary and the pin reciprocates. The pin can be a ball, a hemispherical tipped pin, or a flat-ended cylinder.

Taber Abrasion Test

Test specimens are placed on the abrader turntable and are subject to the rubbing action of a pair of rotating abrasive wheels. Wear

action results when a pair of abrasive wheels is rotated in opposite directions by a turntable on which the specimen material is mounted. The abrading wheels travel on the material about a horizontal axis displaced tangentially from the axis of the test material, which results in a sliding action[44].

Abrasive Belt Test

A flat-ended block of cylindrical specimen is abraded by sliding against an abrasive belt. The belt runs horizontally, while the specimen runs transversely across the belt.

CHAPTER 3 METHODOLOGY

This section describes the methodology implemented to carry out the proposed research to characterize the tribological properties of aluminum matrix composites containing copper and magnesium and reinforced with AlB_2 particles. This includes the material selection, fabrication of the composite, characterization methods, experimental setup and assessment procedure. Figure 3-1 shows a flowchart representing step-by-step the methodology followed.

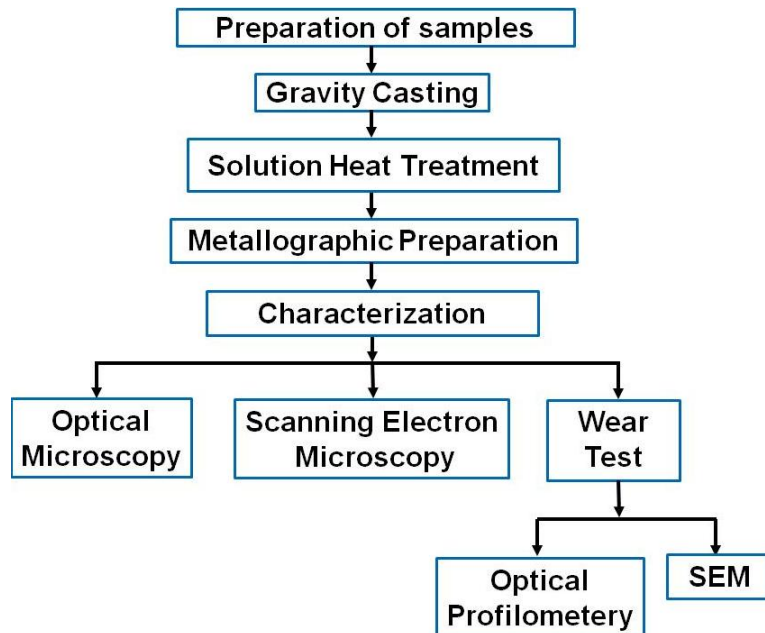


Figure 3-1: Experimental methodology flow chart

3.1 Materials

For the fabrication of the Al-B-Cu-Mg composites, three commercial master alloys were used: Al-5wt.%B, Al-10wt.%Mg and Al-33wt.%Cu. In addition 99%pure aluminum helped set up the balance. Magnesium and copper were used as alloying elements, because of their excellent strengthening of aluminum. AlB_2 particles (contained in the Al-B master alloy), were used as reinforcement in the fabrication of the composite; they had a range in particle size from $1\mu m$ to $20\mu m$ [62], a density of $3.2g/cm^3$, accompanied by high melting point and high hardness[63]. The chemical composition of the AMCs prepared is given in Table 3-1.

Table 3-1: Chemical composition in weight percent of the Al-B-Cu-Mg composites studied

Al- 2.5 wt.% Cu			
wt.% Mg	0	1	3
wt.% B	0	0	0
	1	1	1
	2	2	2
	3	3	3
	4	4	-

The boron levels selected are linearly related to the particle loading (vol. %), as measured by Calderon (Figure 3-2)[64]

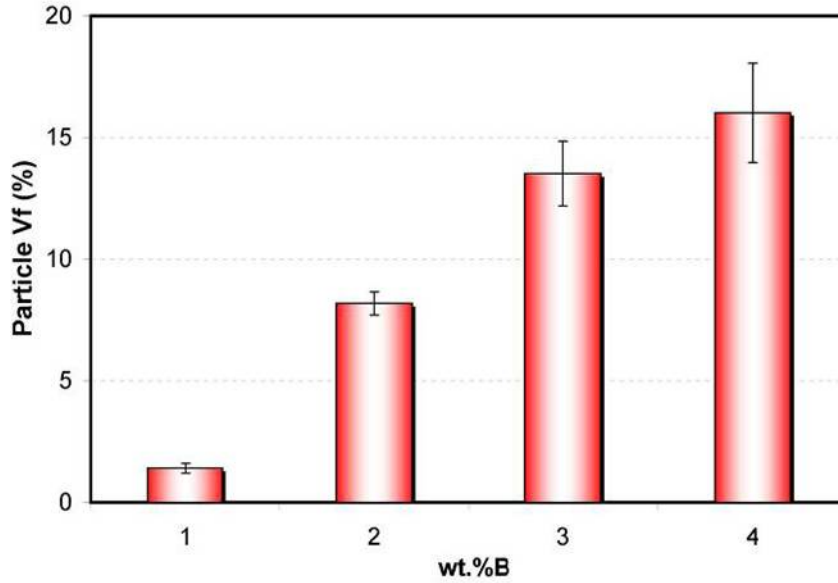


Figure 3–2: Particle volume fraction as function of wt.%B

3.2 Preparation of the Composite

The AMC's reinforced with AlB_2 dispersoids were obtained through gravity casting. To determine the required amount of each master alloy and attained the compositions it needs, a mass balance was employed based on equation 3.1[62].

$$M = \left(\frac{w_f}{w_o} \right) P \quad (3.1)$$

Where, M is the required amount of each alloy (g), P is the final weight of the composites (g), w_f is the element weight % in the composite and w_o is the element weight % in the master alloy.

All the change material, i.e. the master alloys plus the pure aluminum for balance, was melted in a furnace at 750°C . In the process AlB_2 particles remained unchanged because of its higher melting

point, than the aluminum matrix. Since the reinforcements have a higher density (3.2 g/cm^3) than liquid aluminum at the melting furnace temperature ($\sim 2.4 \text{ g/cm}^3$), these tend to be at the bottom of the graphite crucible. Therefore, for the sake of more homogeneity of the samples, manual agitation was applied. The melted material was poured into the cast cylindrical pre-heated graphite mold, used because of its high thermal conductivity (Figure 3-3).

After the cast process, the samples were homogenized via heat treatment (HT) in a resistance furnace. The HT consisted of annealing samples at 350°C for 4 hours and slow cooling in oven down to room temperature. The purpose of this treatment is to homogenize the distribution of the alloying elements in the matrix.

3.3 Metallographic Preparation

The specimens were cut with a low speed saw. Samples were then ground and polished for metallographic analysis. The grinding steps included 320, 400, 600, 800 grit SiC papers. The samples were polished using $3\mu\text{m}$ diamond suspension followed by a $0.05 \mu\text{m}$ SiO_2 emulsion. Finally the samples were cleaned with distilled water and alcohol and dried to be characterized. The samples were then observed using optical and scanning electron microscopy. They were tested with superficial Rockwell hardness, Brinell hardness and pin-on-disk.



Figure 3–3: Mold, graphite crucible and furnace used for composite manufacturing

3.4 Materials Characterization

With the purpose of characterizing the composites and determining their effectiveness in wear resistance, three characterization methods were employed: microstructure analysis, hardness testing and pin-on-disk wear testing.

3.4.1 Microstructure

Examination of the composites microstructures was carried out using optical microscopy and SEM. For optical microscopy, the samples were observed using a Nikon Epiphot 200 inverted optical microscope. Additional microstructure evaluation was performed with a JEOL 6390 scanning electron microscope.

3.4.2 Hardness

When concerned with surface properties of importance to friction and wear processes, measurement of the macro-hardness of the material is a quick and simple method for obtaining mechanical property data. The sample hardness was measured using two different types of tests that are appropriate and relevant to wear in order to increase the reliability of the data. The two techniques are described in the next section:

Superficial Rockwell Hardness

The 15T superficial Rockwell hardness test method used for the Al-B-Cu-Mg composites consists of indenting the material with a 1/16" hardened steel ball indenter and a force of 15kgf, following the ASTM E18 standard. A LECO Rockwell LR-50 hardness tester was used to this purpose (Figure 3-4). To evaluate the experimental data dispersion and reliability at the measured hardness values, twenty tests were conducted on each sample.



Figure 3-4: LECO LR-50 Rockwell hardness testing system

Brinell Hardness

Twenty Brinell hardness tests were performed on each sample using the TH130 Hardness Tester device, shown in Figure 3-5. The measuring method in this instrument is defined as the quotient of the impact body's rebound velocity over its impact velocity. This Brinell test method follows the ASTM E10 standard.



Figure 3-5: TH130 Brinell hardness tester

3.4.3 Pin-on-disk Test

Pin and disk material

The disks were made of the Al-Cu-Mg-B composites samples as explained in the previous chapters, and the samples surfaces were polished using a $0.05 \mu\text{m}$ SiO_2 emulsion. The disk samples had a diameter of 19mm and a thickness of 8mm. The pin (ball) used to produced the wear tracks (scars) was made of 440 martensitic stainless steel with a 3mm diameter.

Experimental Setup

The pin-on-disk test apparatus was custom made (Figure 3-6). It was used to investigate the dry sliding wear characteristics of the composite. The apparatus design was based on the ASTM G99 standard. The setup consist of a stationary pin, which rest on a rotating disk under the influence of a dead weight. Paramenters such as normal load, rotational speed and wear track diameter are factors to be set before running the tests.

Experimental Procedure

Wear testing for the Al-B-Cu-Mg composite samples were carried out in air at room temperature. For the pin-on-disk technique, the spherical pin was held stationary against the composite rotating disk, as shown in Figure 3-7. A track diameter of 3.5mm was fixed for all tests. The tests were conducted with a constant load of 1N at a sliding speed of 0.004m/s and a contact sliding distance of 2.5 m. Samples were tested twice at each condition and the average wear volume and rates were calculated. The wear rate was defined as the ratio of the wear volume to sliding distance. The worn surfaces and wear debris were analyzed using a SEM (furbished with a EDS system), optical microscopy and optical profilometry.

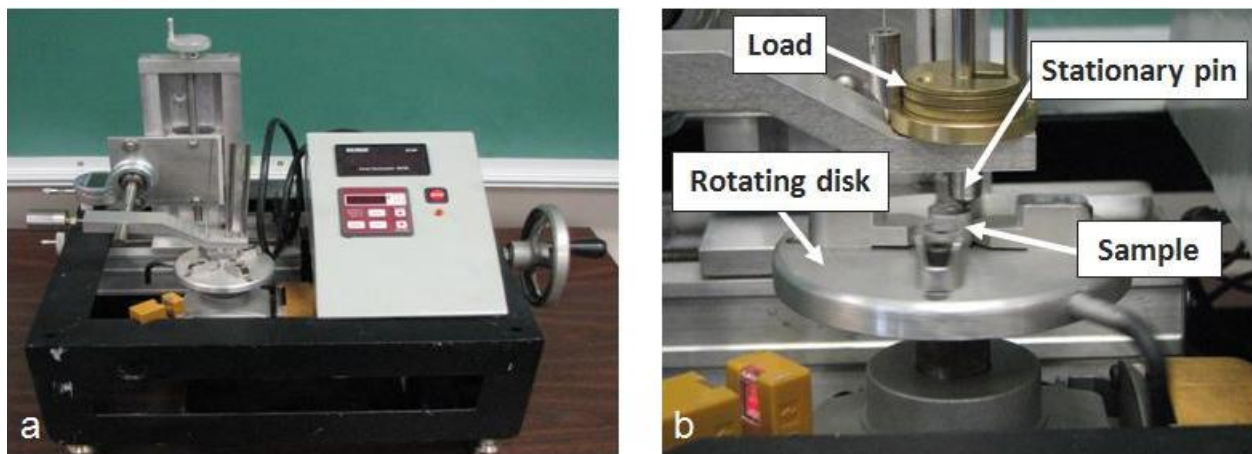


Figure 3-6: a) Pin-on-disk test apparatus constructed at UPRM, b) Components of pin-on-disk test apparatus

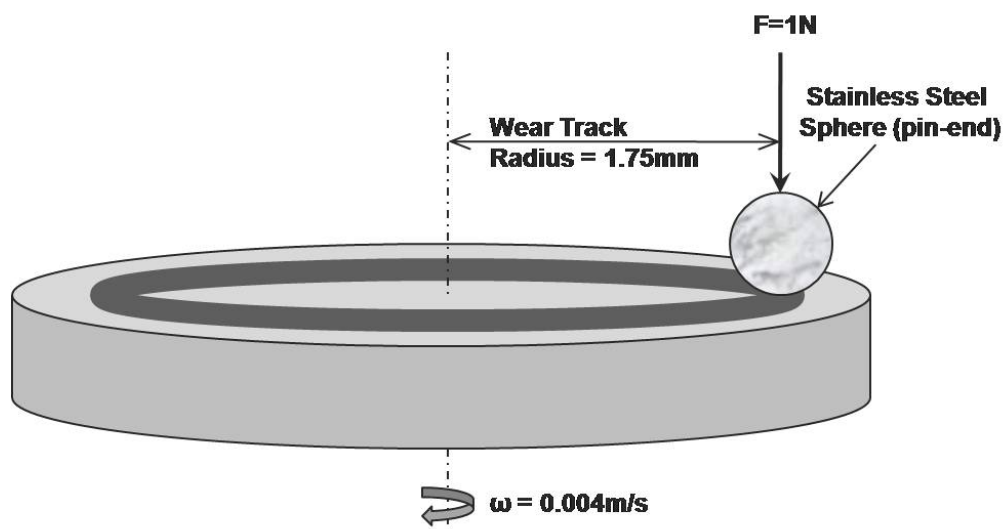


Figure 3-7: Schematic view of pin-on-disk measuring system applied

CHAPTER 4

COMPOSITES CHARACTERIZATION

RESULTS AND DISCUSSIONS

4.1 Microstructure Analysis

4.1.1 Optical Microscopy

The composite microstructure for each sample was analyzed at different magnifications. Figure 4-1 presents the resulting microstructure of the Al-2.5%Cu-1%Mg-2%B composite showing AlB_2 particles embedded in the aluminum matrix. Figure 4-2 evince the AlB_2 particles are distributed in clusters throughout the entire matrix. Figure 4-3 evinces a higher concentration of reinforcement particles in the matrix while boron levels increases in the composite. In Figure 4-3a, the intermetallic phase, Al_2Cu (θ) is apparent throughout the matrix but mainly in grain boundaries[62].

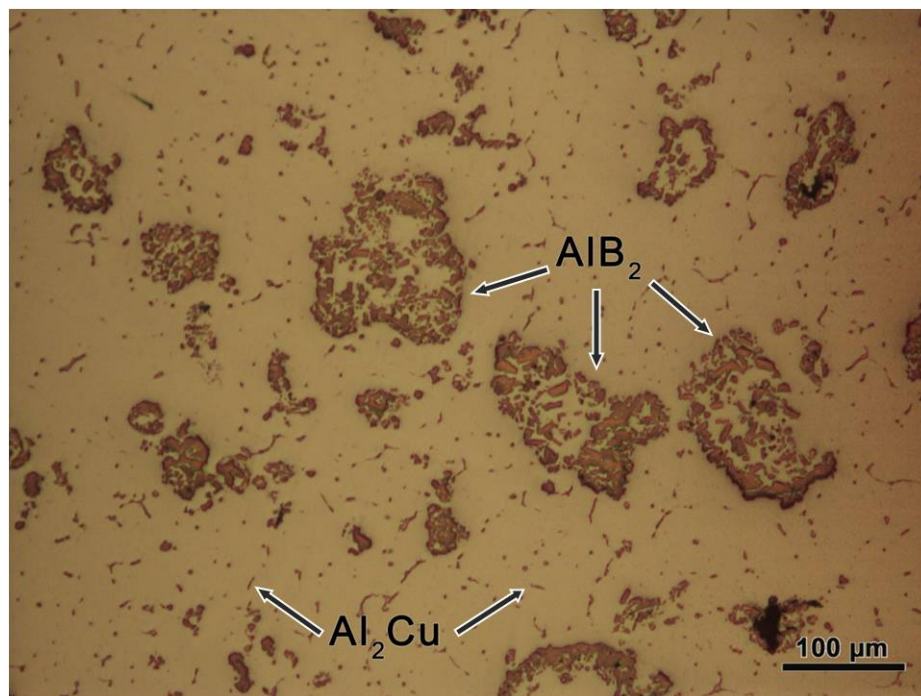


Figure 4-1: Microstructure of Al-2.5%Cu-1%Mg-2%B composite

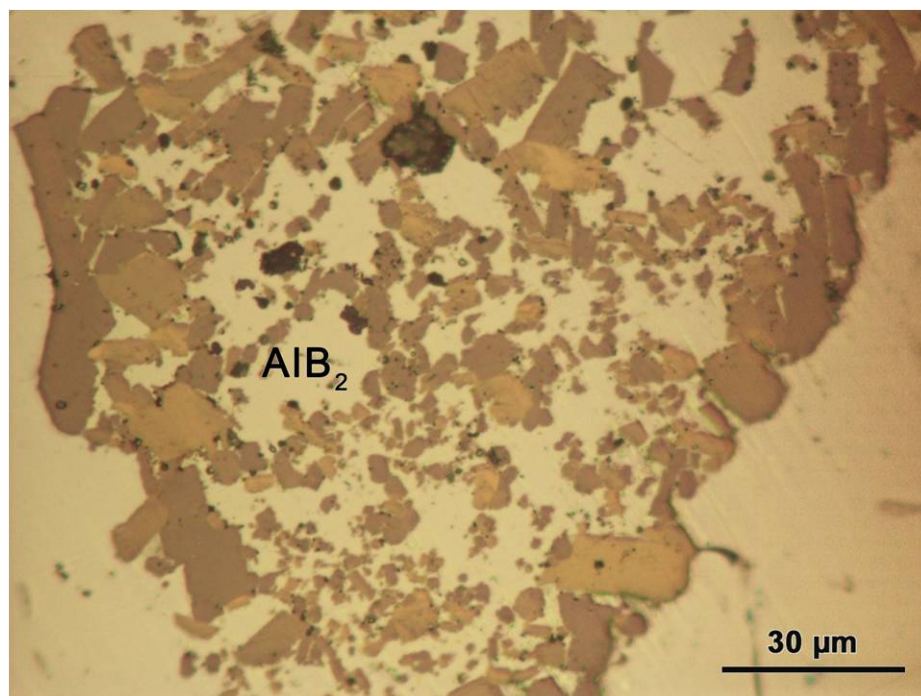


Figure 4-2: AlB_2 cluster shown at higher magnification in Al-2.5%Cu-3%Mg-3%B composite

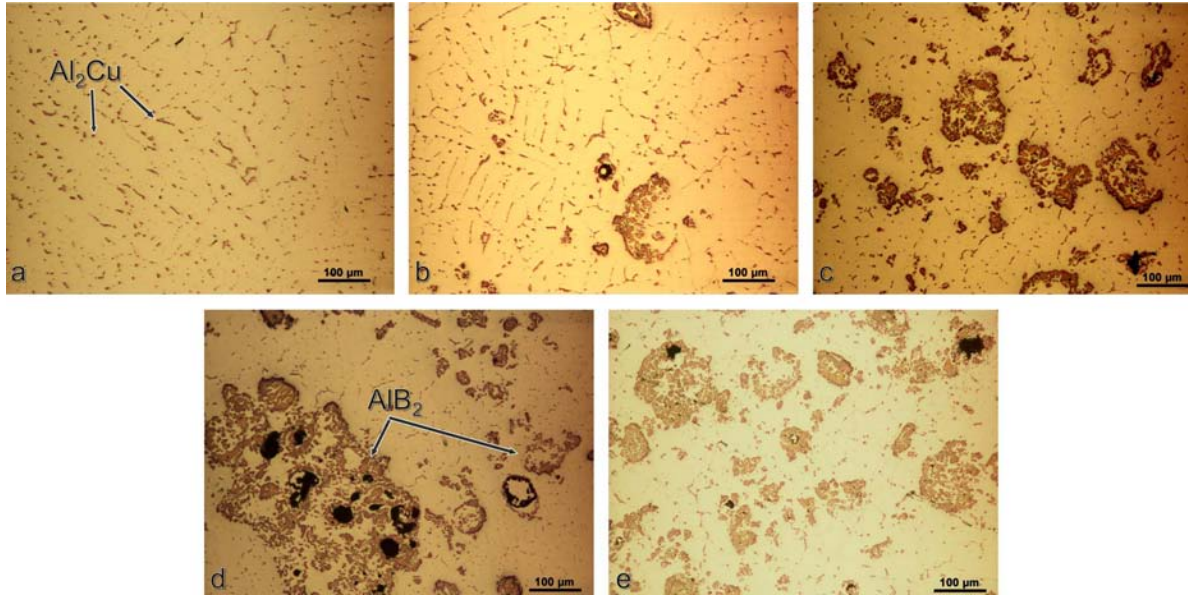


Figure 4-3: Optical micrographs showing the AlB_2 distribution while boron levels increases from 0 wt.% to 4 wt.% a) Al-2.5%Cu-1%Mg-0%B, b) Al-2.5%Cu-1%Mg-1%B, c) Al-2.5%Cu-1%Mg-2%B, d) Al-2.5%Cu-1%Mg-3%B, e) Al-2.5%Cu-1%Mg-4%B

4.1.2 Scanning Electron Microscopy (SEM)

The samples were observed in the SEM along with the energy dispersive spectroscopy (EDS) to corroborate the presence of aluminum, boron, copper and magnesium in the composite, as shown in Figure 4-4. Figure 4-4a shows the microstructure of Al-2.5% Cu-1% Mg-2% B composite, where an elliptical cluster of AlB_2 can be observed, while Figure 4-4b shows a global EDS spectrum, revealing the presence of copper, magnesium and aluminum in the Al-2.5% Cu-1% Mg-2% B composite. By using x-ray mapping which allows detecting relative chemical composition in the composite, the distribution of Cu and Mg can be shown. Cu appears uniformly distributed throughout the matrix (Figure 4-5). Although, the mapping of magnesium shows a

uniform distribution in the matrix, a higher Mg concentration appears surrounding the AlB_2 reinforcements, as shown in Figure 4-6.

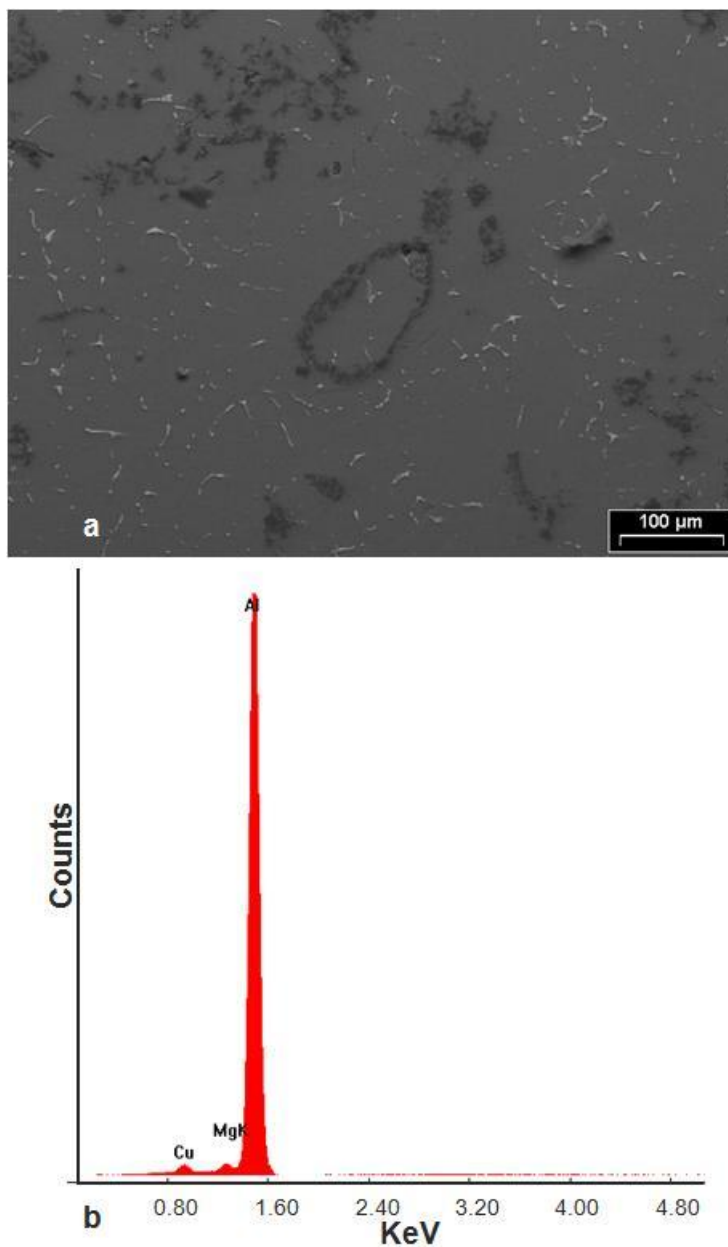


Figure 4-4: a) SEM image of Al-2.5%Cu-1%Mg-2%B, b) Global EDS spectrum of the worn surface detected in Al-2.5%Cu-1%Mg-2%B composites

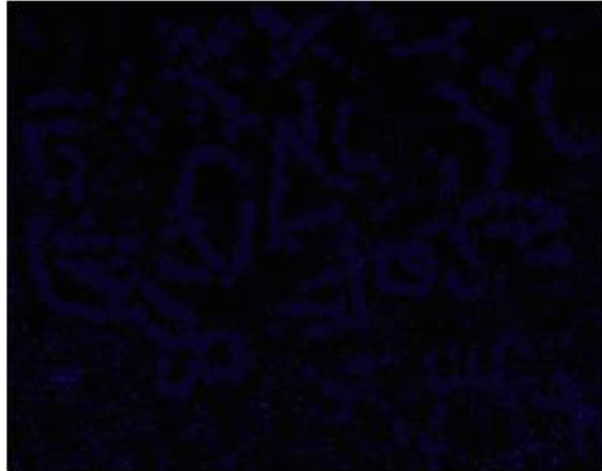


Figure 4-5: EDS mapping analysis of Cu on the surface of Al-2.5%Cu-1%Mg-2%B composite

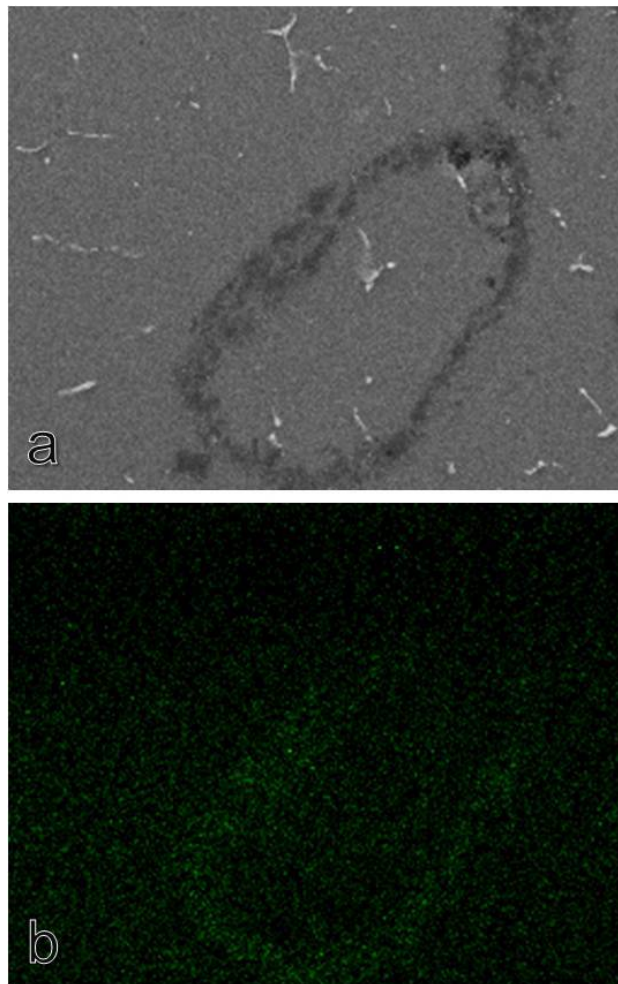


Figure 4-6: Al-2.5%Cu-1%Mg-2%B sample a)SEM micrograph b)EDS elemental map of magnesium

4.2 Hardness Study

4.2.1 Superficial Rockwell Hardness

Figure 4-7 shows the variation of superficial Rockwell hardness (HRS 15T) of the composites as function of the amount of AlB_2 reinforcements present in the samples. In a metal matrix composite one should have expected an enhancement in hardness with increasing concentration of borides in the sample. However, our results revealed different tendencies for the different composites. Samples containing Mg showed a decreasing tendency in the superficial hardness as the level of boron increased. On the other hand, samples without Mg showed a hardness increment with the percentage boron, as shown in Figure 4-7. It is suspected that such hardness drop in the Mg-containing samples is a consequence of an interaction between AlB_2 particles and the Mg. These unexpected results were verified and were repeatable enough, showing the same trend all over again. This strong influence open new research tasks to understand the nature of the interaction of Mg into the diborides.

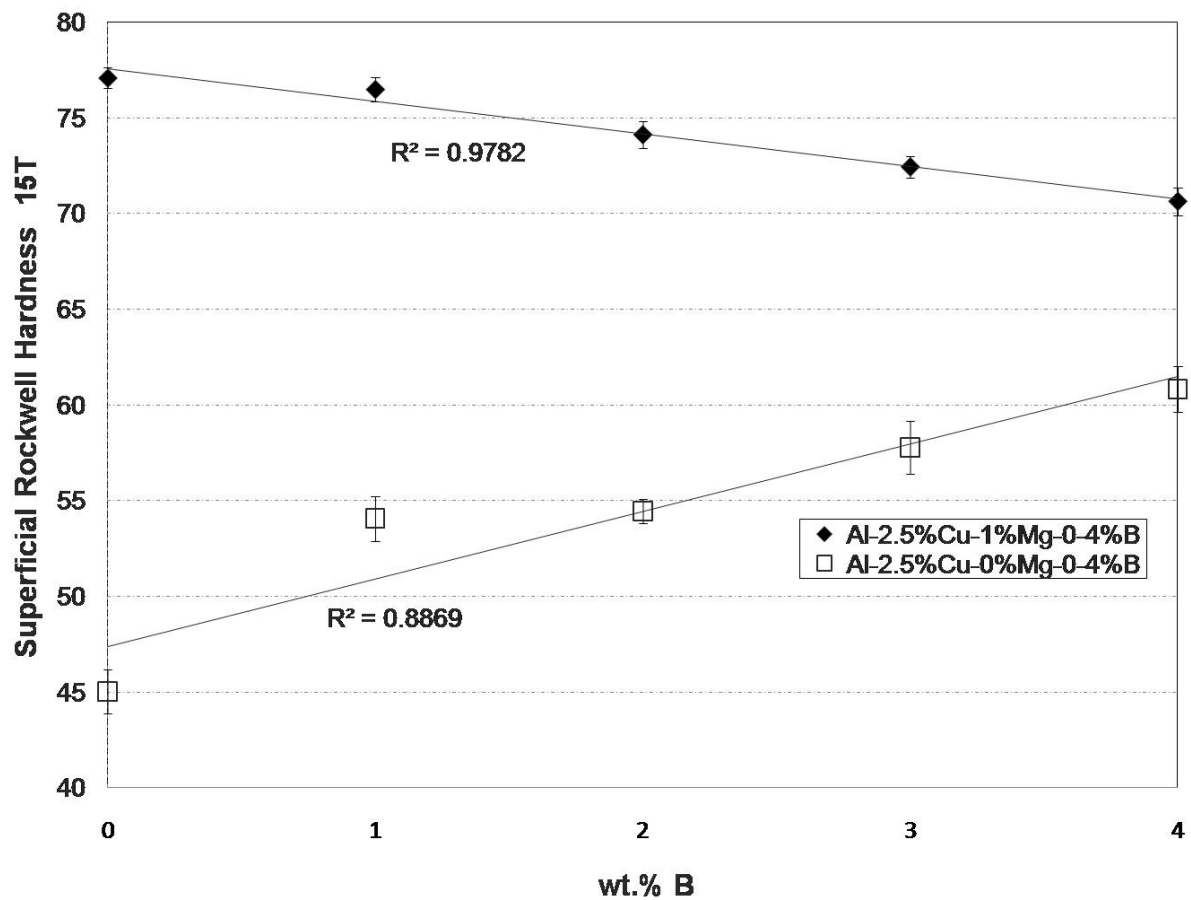


Figure 4-7: Superficial Rockwell hardness (HRS 15T)

4.2.2 Brinell Hardness

The results achieved through Brinell hardness are in agreement with those of superficial Rockwell hardness. Samples containing magnesium presented a decrease in hardness as a function of boron, while in samples containing no magnesium, Brinell increases with the amount of diborides (Figure 4-8).

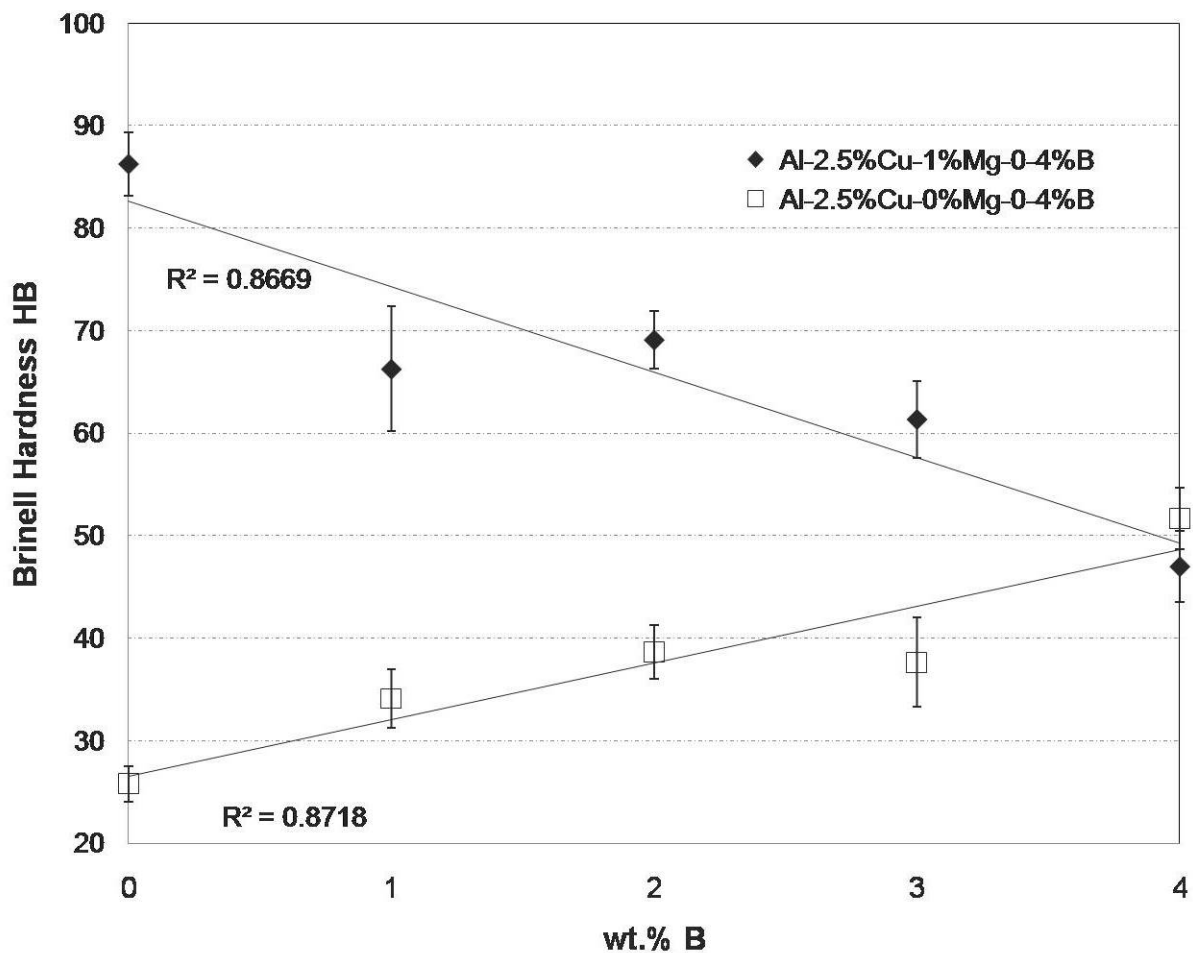


Figure 4-8: Brinell hardness (HB)

4.3 Tribological Testing Analysis

4.3.1 Pin-on-disk Test

Tribological experiments were focused on the determination of the degree of wear measured by the material volume removed and the wear coefficient value. These variables were then correlated to the amount of boron present in the composite. The wear behavior of the samples was evaluated by implementing a pin-on-disk test, as discussed in a previous chapter.

4.3.2 Wear Characteristics

A primary concern with wear tests is the actual measurements of wear. Common wear measurements include volume loss, displacement scar width and depth and wear coefficients. Preferably, wear measurement methods should reproduce the actual service performance of the system. It should be repeatable and as objective as possible. For this research the wear measurement method consisted of the calculation of wear volume and wear coefficient for each composite.

Wear Volume

This research focuses on methods based on topographical analysis, taking into consideration the track width, depth and perimeter. These parameters allowed the calculation of wear volume on each sample. The volume loss calculated by this means may contain certain error

due to variations around the wear track, accumulations of debris and plastic deformation in our material. For this reason and based on the ASTM G99 standard, changes in measures of length and depth of the disk wear track are determined by any suitable metrological technique, such as electronic distance gaging or profiling techniques. This method is frequently used because it provides more accurate measurements of the disk wear volume, since mass loss is often too small to measure precisely[65].

The worn surface was evaluated using a 3-D optical Zygo New View 6300 profilometer system (Figure 4-9) to obtain the maximum depths of the wear tracks and their widths. This interference microscope allows non-destructive examination. The system is based on scanning white-light interferometry resulting in a 3-D image[66]. To analyze the wear track, 3-D profile images were taken at six representative locations on the sample surface, as shown in Figure 4-10. The average values from the six locations of the depth and width of the wear track of each sample were determined and are shown in Table 4-1. The standard deviations of the depth and width of the wear track indicate that the shape of the wear track is often not regular.



Figure 4-9: 3-D optical Zyo New View 6300 profilometer system

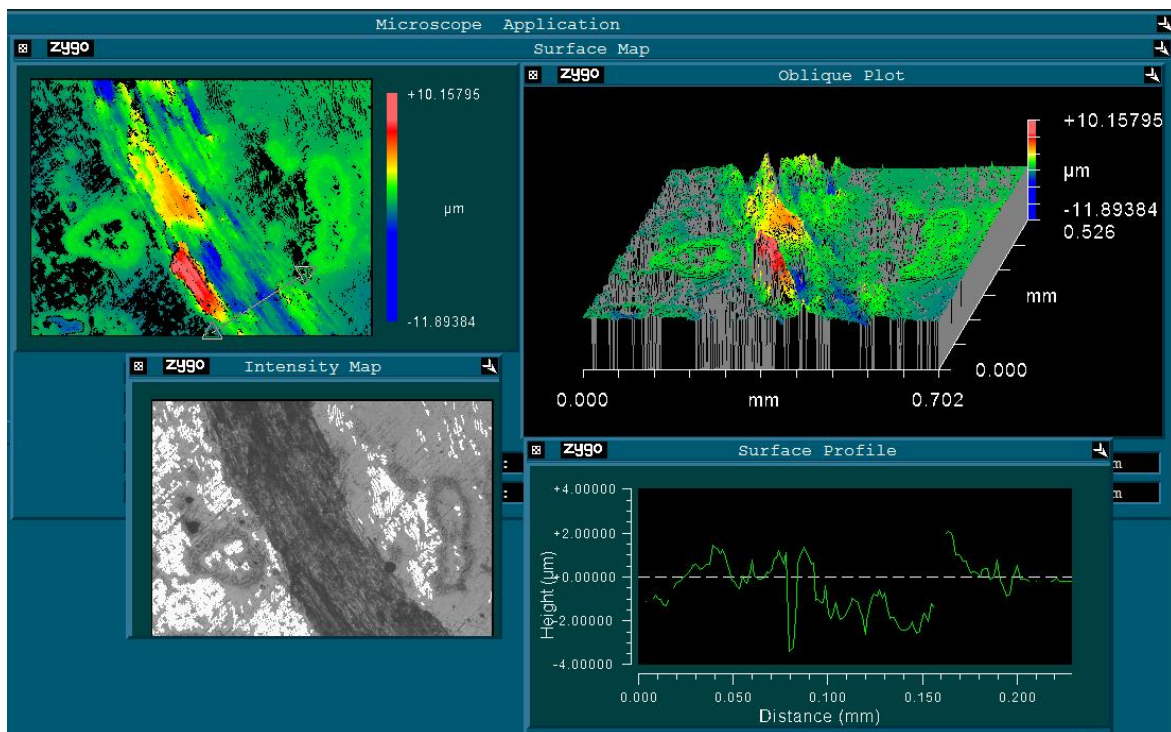


Figure 4-10: 3-D profile image of Al-2.5%Cu-3%Mg-2%B sample

Table 4-1: Average values of the depth and width of wear track for each sample measured with the optical profilometer

Sample	Depth (μm)	Width (mm)
Al-2.5%Cu-0%Mg-0%B	6.23 \pm 1.07	0.319 \pm 0.02
Al-2.5%Cu-0%Mg-1%B	5.86 \pm 0.61	0.256 \pm 0.02
Al-2.5%Cu-0%Mg-2%B	4.93 \pm 0.49	0.261 \pm 0.01
Al-2.5%Cu-0%Mg-3%B	2.60 \pm 0.32	0.240 \pm 0.01
Al-2.5%Cu-0%Mg-4%B	2.46 \pm 0.30	0.236 \pm 0.01
Al-2.5%Cu-1%Mg-0%B	5.73 \pm 0.56	0.391 \pm 0.01
Al-2.5%Cu-1%Mg-1%B	5.66 \pm 0.79	0.319 \pm 0.01
Al-2.5%Cu-1%Mg-2%B	5.82 \pm 0.40	0.289 \pm 0.01
Al-2.5%Cu-1%Mg-3%B	5.28 \pm 0.99	0.271 \pm 0.01
Al-2.5%Cu-1%Mg-4%B	2.85 \pm 0.69	0.183 \pm 0.01
Al-2.5%Cu-3%Mg-0%B	5.24 \pm 0.46	0.273 \pm 0.01
Al-2.5%Cu-3%Mg-1%B	4.71 \pm 0.71	0.267 \pm 0.005
Al-2.5%Cu-3%Mg-2%B	3.69 \pm 0.55	0.229 \pm 0.01
Al-2.5%Cu-3%Mg-3%B	3.26 \pm 0.77	0.181 \pm 0.02

The parameters obtained by the 3-D profile images allowed calculating the wear volume on each sample. Figure 4-11 shows the variation of wear volume as a function of boron levels. Clearly, as the levels of boron increases, the wear volume decreases. The wear volume of the unreinforced alloy is greater than their composites containing diboride particles. We conclude that wear volume is decreasing with the addition of AlB_2 particles. In general, the lowest wear volume measured was observed on the composites containing 4%B.

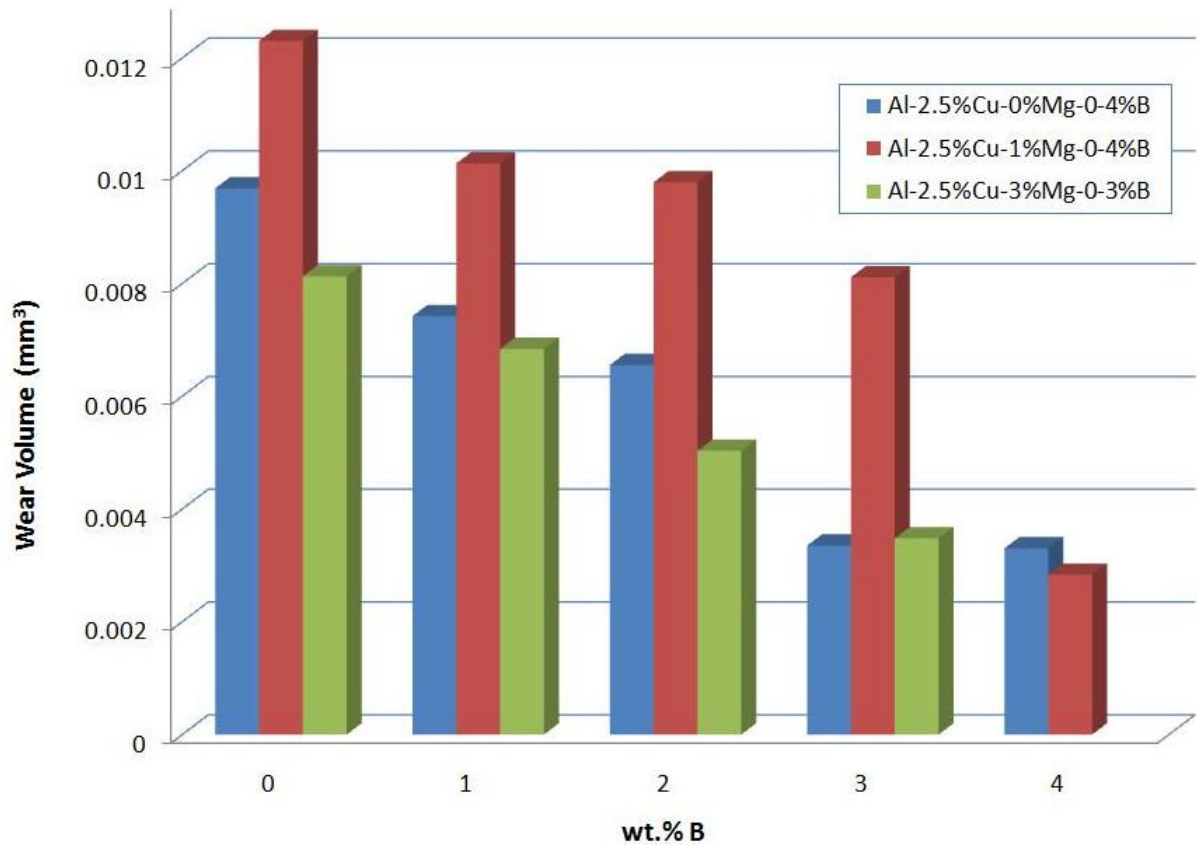


Figure 4-11: Wear volume as function of boron percentage in the samples

If we take the time taken for the wear volume, we can calculate the removal rate (RR) using Preston equation (Equation 2.2). Removal rate is a very important parameter in many tribological test like chemical-mechanical planarization (CMP). Table 4-2 shows the variation of RR as a function of boron levels, showing the same tendencies of wear volume.

Table 4-2: Removal Rate (mm^3/s) as function of boron percentage in the samples

Sample	Removal Rate(mm^3/s)
Al-2.5%Cu-0%Mg-0%B	1.6145×10^{-5}
Al-2.5%Cu-0%Mg-1%B	1.2367×10^{-5}
Al-2.5%Cu-0%Mg-2%B	1.0921×10^{-5}
Al-2.5%Cu-0%Mg-3%B	5.5863×10^{-6}
Al-2.5%Cu-0%Mg-4%B	5.5050×10^{-6}
Al-2.5%Cu-1%Mg-0%B	2.0501×10^{-5}
Al-2.5%Cu-1%Mg-1%B	1.6882×10^{-5}
Al-2.5%Cu-1%Mg-2%B	1.6326×10^{-5}
Al-2.5%Cu-1%Mg-3%B	1.3528×10^{-5}
Al-2.5%Cu-1%Mg-4%B	4.7253×10^{-6}
Al-2.5%Cu-3%Mg-0%B	1.3543×10^{-5}
Al-2.5%Cu-3%Mg-1%B	1.1401×10^{-5}
Al-2.5%Cu-3%Mg-2%B	8.3893×10^{-6}
Al-2.5%Cu-3%Mg-3%B	5.8007×10^{-6}

Wear Coefficient

The wear coefficient can be used to compare the performance of materials under the identical operating conditions. For all the composites under same testing conditions, the values of the wear coefficient were calculated based on the worn volume obtained with the parameters measured with the optical profilometer. The wear coefficient of the composites was evaluated using the wear equation (Equation 2.1) proposed by Archard, and explained in Chapter 2. The variation of experimental wear coefficient as a function of boron is shown in Figure 4-12. All composites exhibited similar behavior with the increased

content of AlB_2 , where the wear coefficient decreases in the composites, obtaining higher wear resistance. This behavior is clearly related to the wear volume measured.

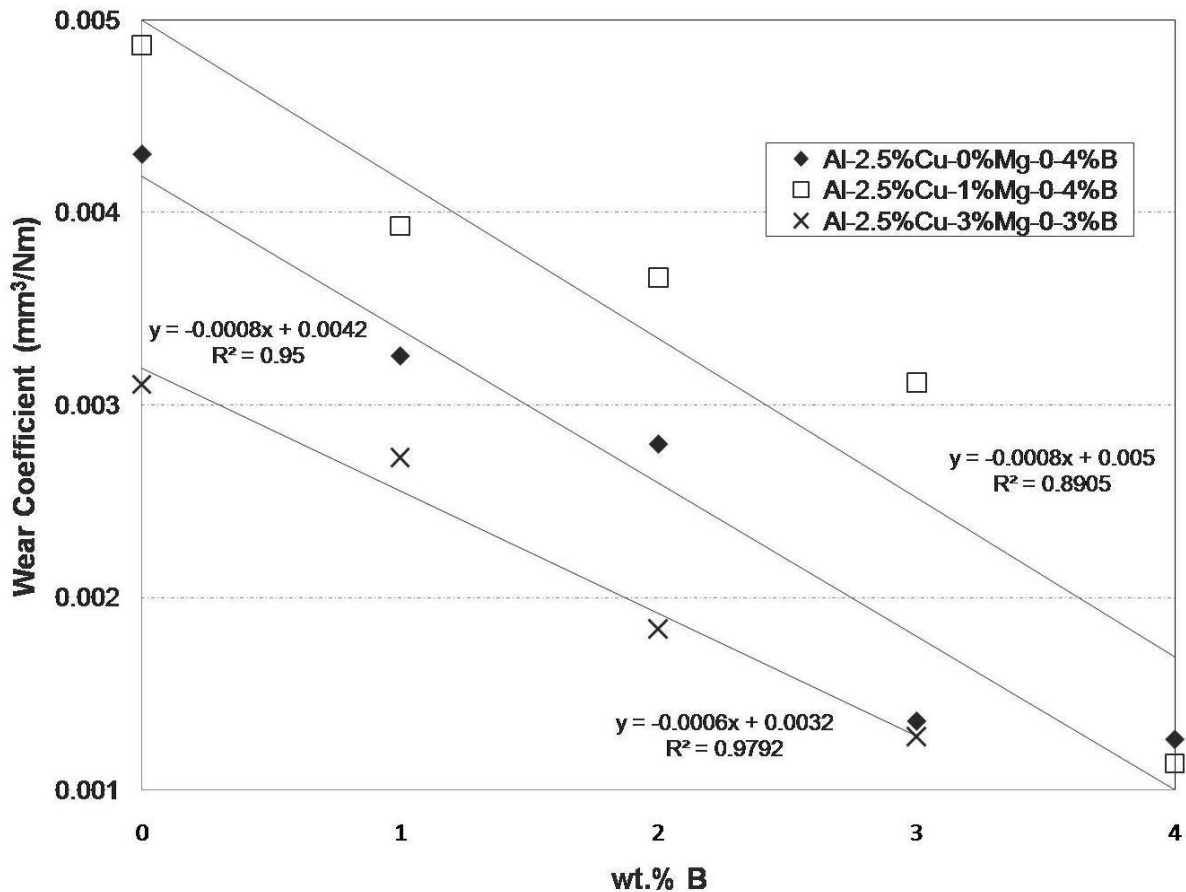


Figure 4-12: Values of wear coefficient of the tested samples versus the AlB_2 particles

4.3.3 Characterization of Wear

Wear mechanisms can be identified and studied by three possible methods: examination of wear debris, visual examination of worn surfaces, and metallographic examination of the worn surface. In the examination of the wear debris, large lumps imply adhesive wear; fine

particles, oxidative wear; chip particles, abrasive wear; and flake particles, delamination wear[67]. In the examination of the worn surface heavy tearing implies adhesive wear; scratches, abrasive wear; and burnishing, nonadhesive wear. Metallographic examination of the surface structure may reveal the type of deformation, the generation of subsurface crack, among other things[67].

Examination of Worn Surfaces

In the present research we examined the wear tracks and wear debris to investigate the wear mechanisms responsible for the composites wear behavior of the composites by means of optical microscopy, optical profilometry and SEM in conjunction with EDS and elemental X-ray mapping. Figure 4-13 shows micrographs of the worn surfaces of the composites using a Nikon SMZ 1500 stereoscope (Figure 4-13a) to perceive the whole track and a Nikon Epiphot 2 inverted optical microscope (Figure 4-13b) to obtain a track magnification. Optical microscope examinations showed parallel scratches with plastic deformation edges. Samples with low content of AlB_2 , as in Figure 4-14a, display a relatively smooth surface morphology with parallel grooves inside the wear track, resulting in a larger depth. Conversely, for composites with higher loading of reinforcement, the worn surface of the sample appears rough, with a smaller measured track depth (Figure

4-14b). The high surface roughness with deep ridges may be due to high friction rather than catastrophic thermoplastic deformation.

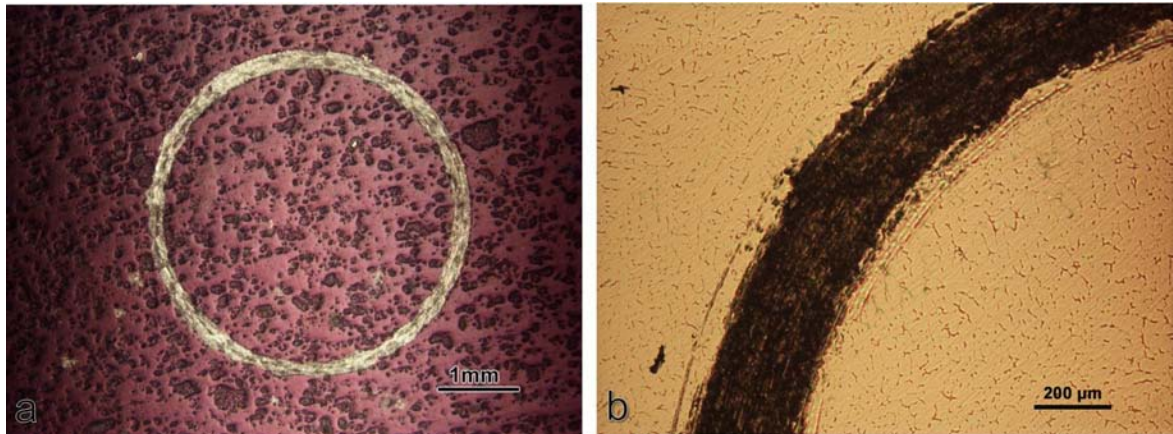


Figure 4-13: Optical micrographs of wear tracks of a)Al-2.5%Cu-3%Mg-2%B composite, b)Al-2.5%Cu-3%Mg-0%B composite

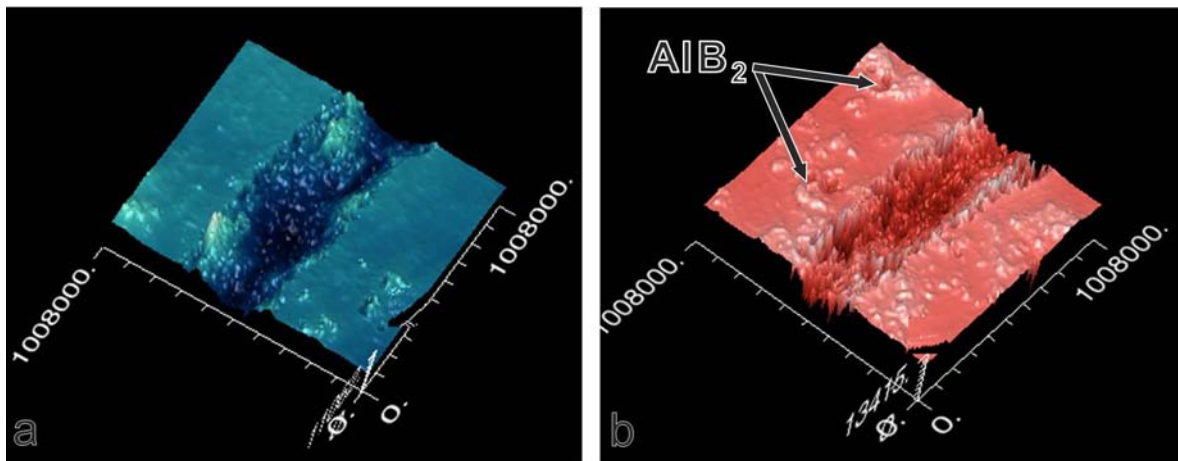


Figure 4-14: 3-D Optical profiler of wear track a)Al-2.5%Cu-1%Mg-1%B, b)Al-2.5%Cu-1%Mg-4%B composite

SEM examination permitted obtaining detailed information of the wear tracks and debris. Figure 4-15 shows the change in widths of the wear track as function of boron percentage in the samples. To get a better idea, in Figure 4-16 the composites wear track width is getting smaller while the level of boron increases. This can be translated in

enhancement of wear resistance in the composites. Moreover, Figure 4-17 present the irregular shape of the wear track with many grooves along the sliding direction while the peeling of the matrix formed worn chips adhered on the composite surface.

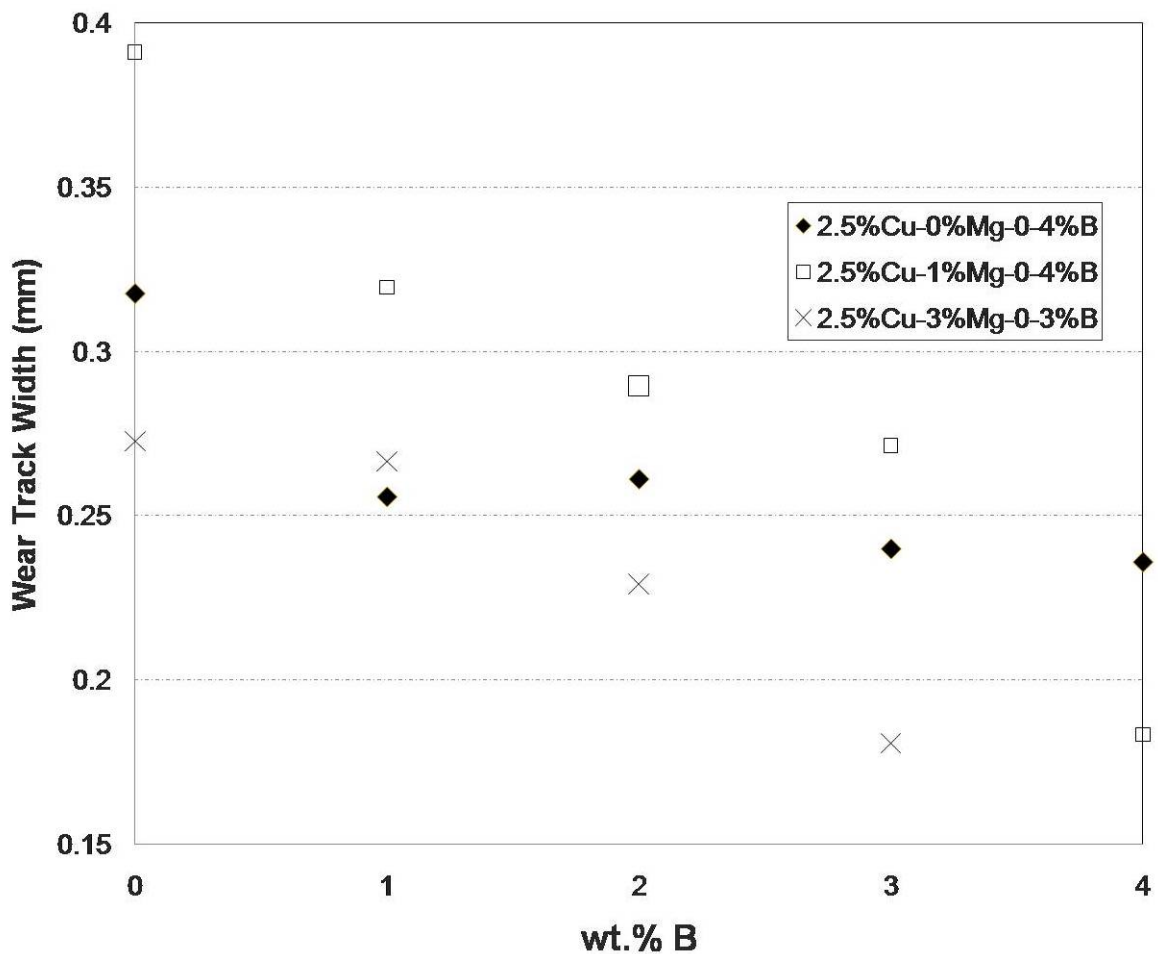


Figure 4–15: Wear track width as function of AlB₂ particles

The SEM observations revealed that the pin-on-disk wear test carried out on the Al-Cu-Mg-B composites induced plastic deformation, ploughing, transfer and deposition of debris to the surface. Hence, the

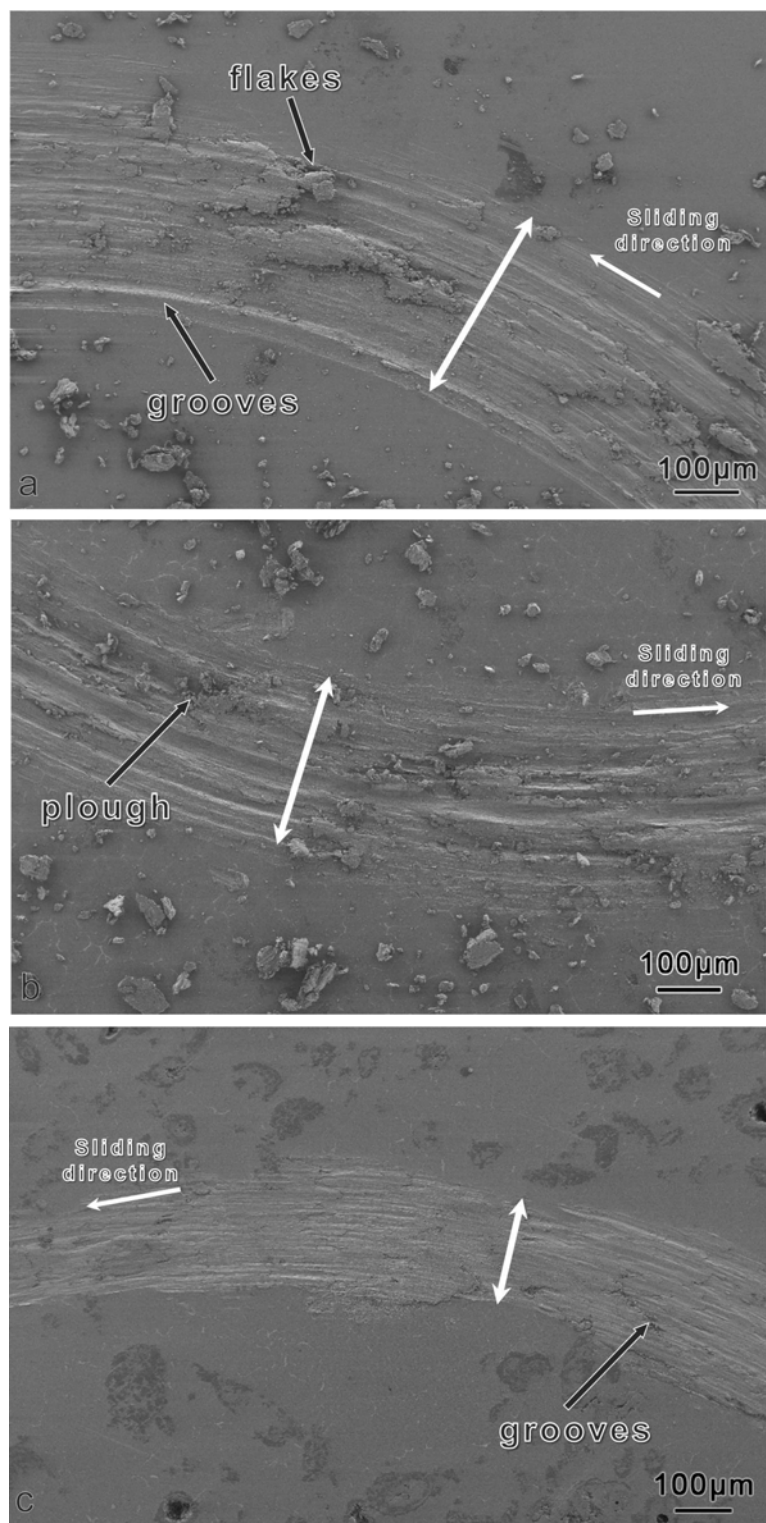


Figure 4-16: SEM micrographs of wear track illustrating grooves, ploughs and debris for identical testing conditions a) Al-2.5%Cu-1%Mg-0%B composite, b) Al-2.5%Cu-1%Mg-3%B composite, c) Al-2.5%Cu-1%Mg-4%B composite

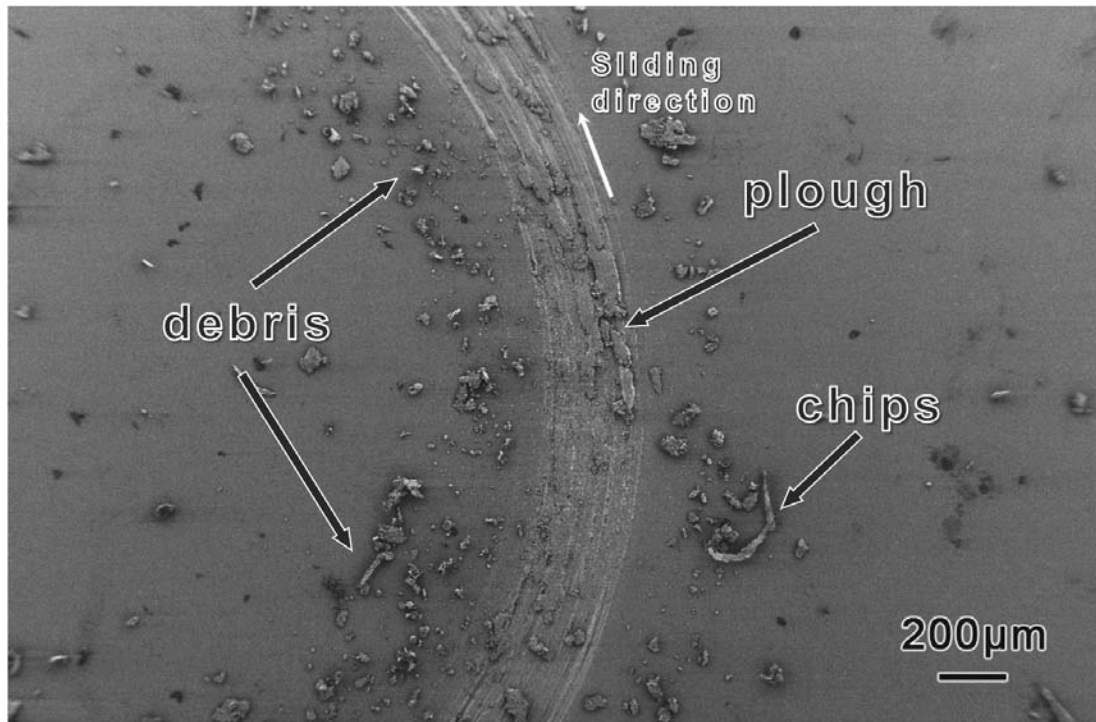


Figure 4-17: SEM micrographs of pin-on-disk track on Al-2.5%Cu-1%Mg-0%B composite

loss of material in the composites is produced by diverse wear mechanisms. The different wear mechanisms identified are: oxidative wear, abrasion wear, and fatigue wear.

Wear Mechanisms

Oxidative Wear. Images of the wear tracks observed using SEM consisted of dark areas where agglomerations of detached flakes are detected as in Figure 4-18. The chemical composition of the surface composites was analyzed using EDS, which coupled with SEM permitted direct elemental analysis of the wear surface as well as

the wear debris. Acquired EDS spectra evinced the presence of oxygen on the worn samples (Figure 4-19). In Figures 4-20 x-ray mapping analysis shows concentration of oxygen in the debris, coinciding with the aforementioned dark areas. These characteristics indicate oxidative wear mechanism, in which unlubricated conditions of sliding causes relatively high "hot-spot" temperatures at the surface producing oxidation[43]. In Figure 4-21 the presence of oxides is revealed in the worn surface.

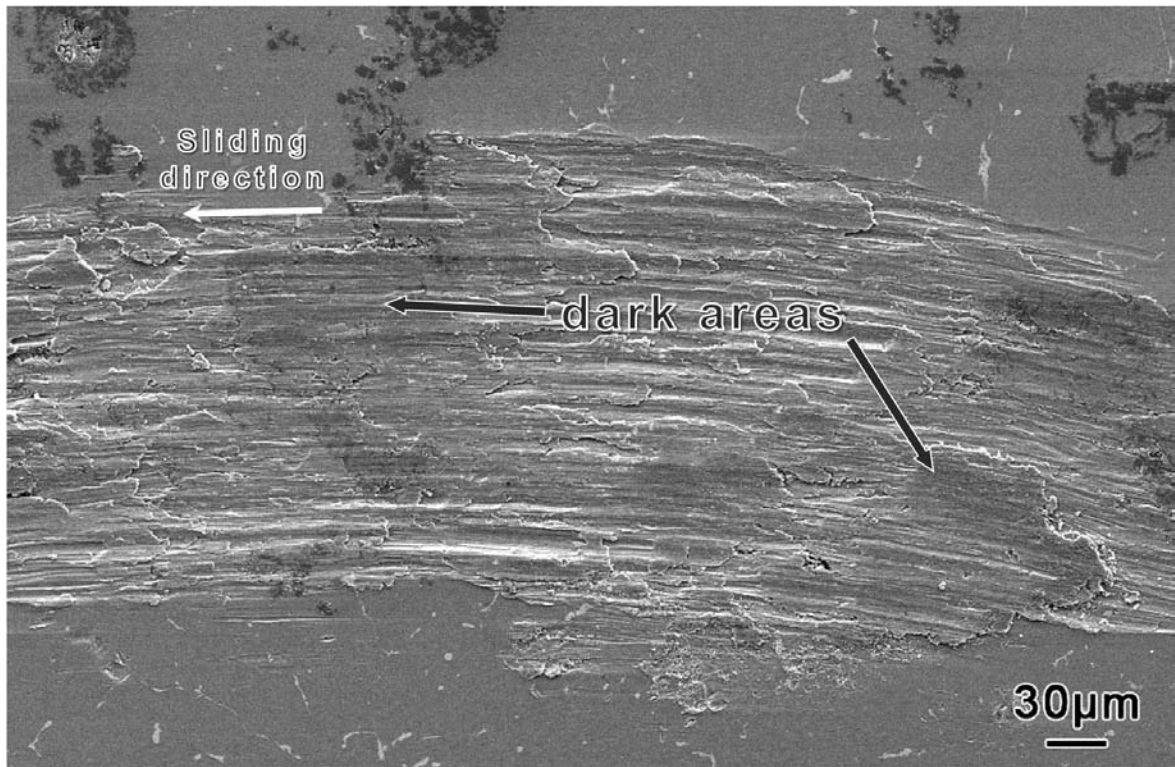


Figure 4-18: SEM micrograph showing the dark areas analyzed by EDS in Al-2.5%Cu-1%Mg-4%B composite

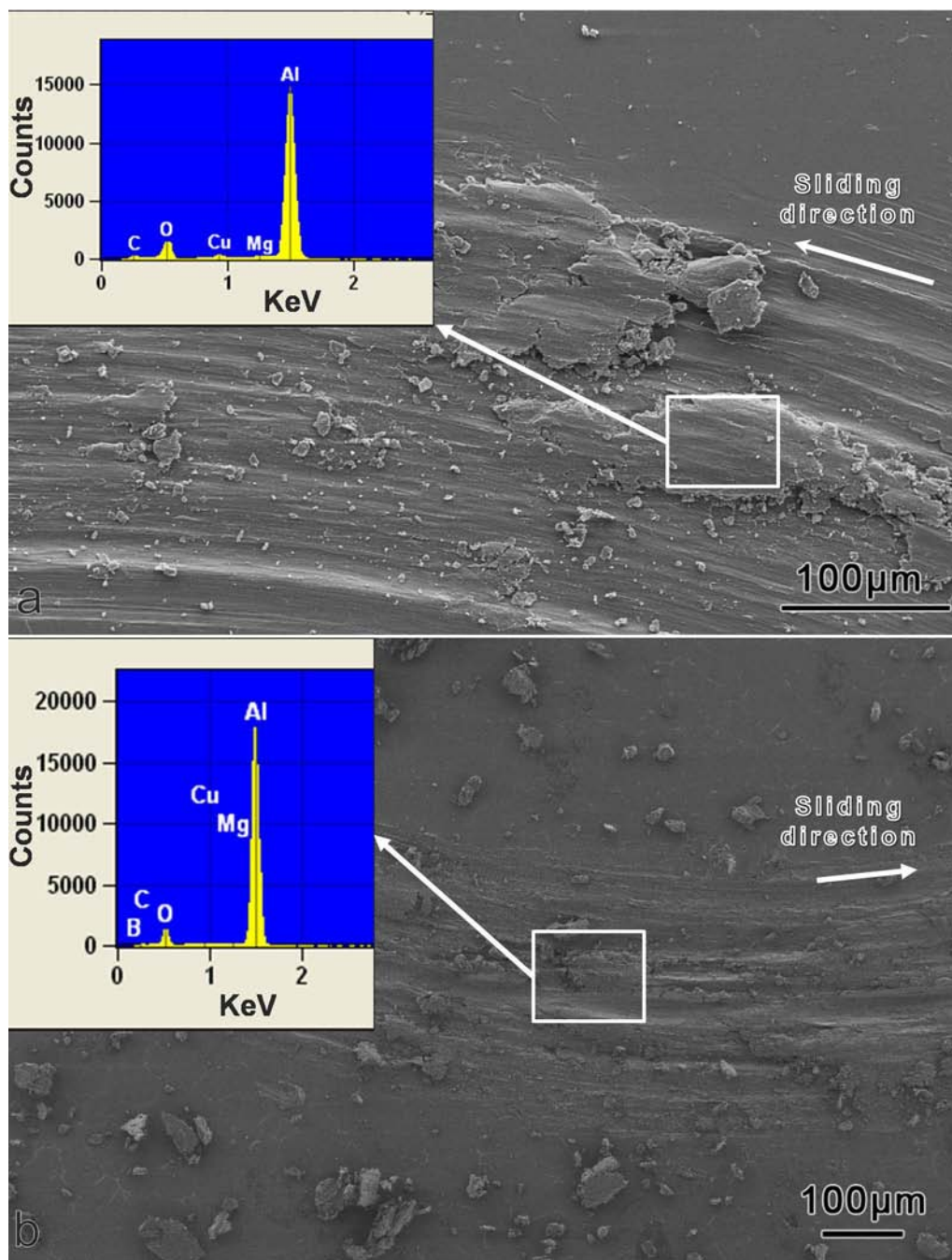


Figure 4-19: EDS spectrum analysis of wear track: a) Al-2.5%Cu-1%Mg-0%B composites, b) Al-2.5%Cu-1%Mg-3%B composite

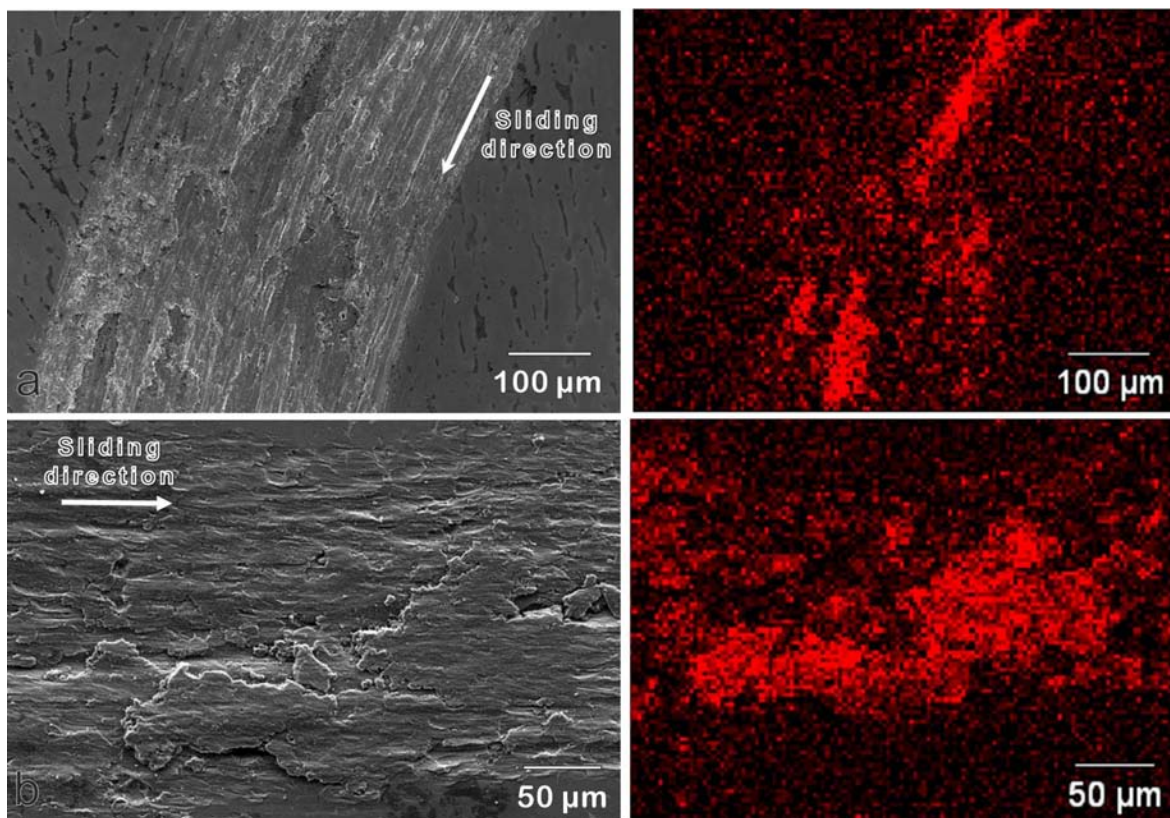


Figure 4-20: SEM micrographs and Oxygen elemental maps of: a) Al-2.5%Cu-3%Mg-0%B, b) Al-2.5%Cu-3%Mg-3%B

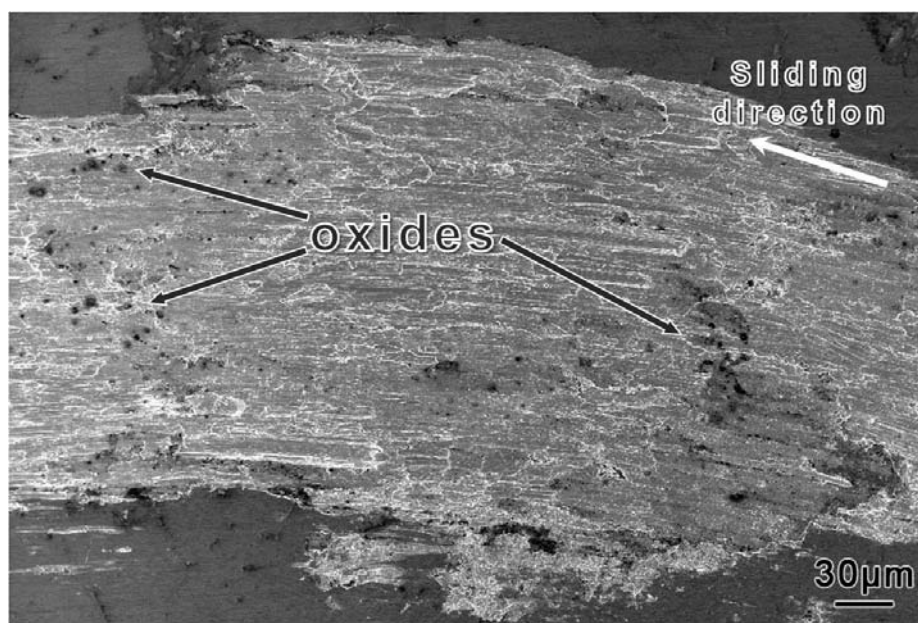


Figure 4-21: SEM image of Figure 4-17 showing the oxides in the worn surface

Abrasive Wear. Figure 4-22 illustrate the appearance of grooving and scratching on the worn surface of the composites, matching the sliding direction. In addition, damage spots forming ploughs were observed in different areas of the wear track (Figure 4-23). Image analysis corroborates the abrasive wear by features related to the material removed from the surface of a component by a cutting action and displaced on either side of the abrasion groove[68].

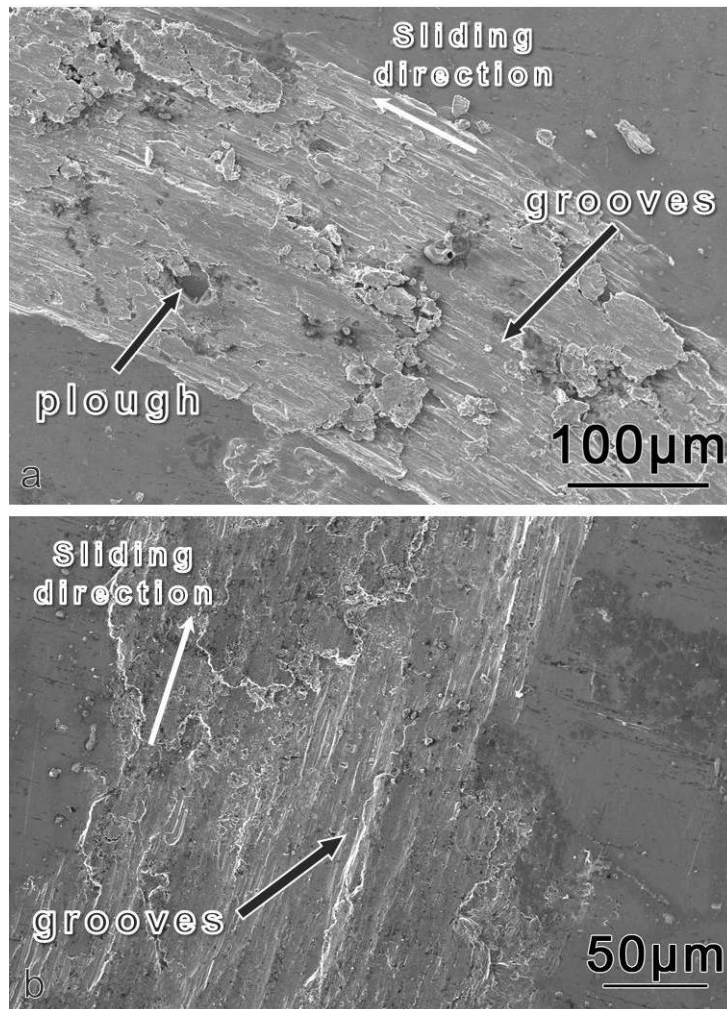


Figure 4-22: SEM micrographs showing grooves due to abrasive wear: a) Al-2.5%Cu-0%Mg-1%B composite and b) Al-2.5%Cu-0%Mg-3%B composite

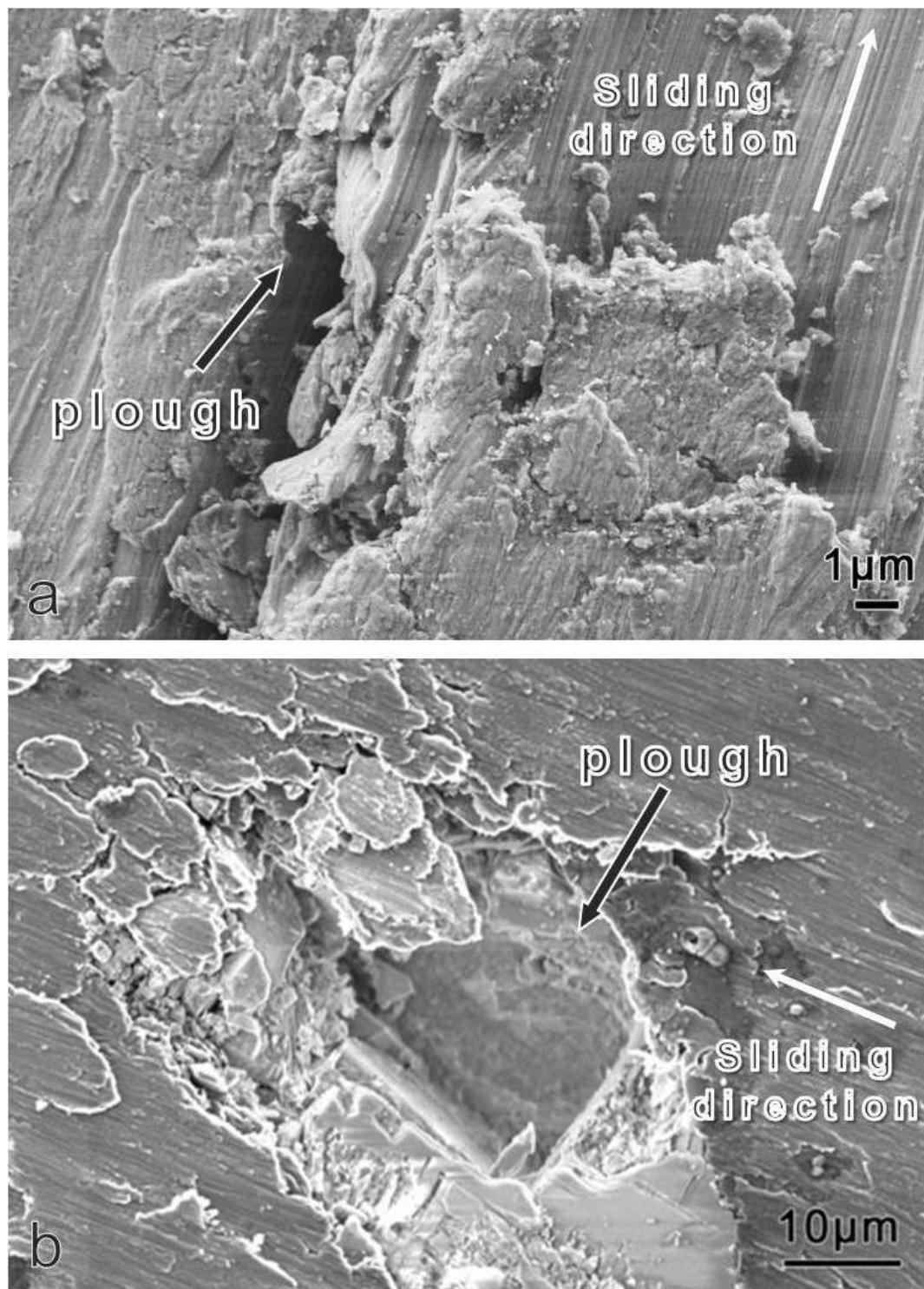


Figure 4-23: Ploughing effects observed using SEM for: a) Al-2.5%Cu-3%Mg-0%B composite b) Al-2.5%Cu-0%Mg-1%B composite

Delamination Wear. According to the SEM images, there is evidence of delamination wear on the composites surface (Figure 4-24). Delamination wear is an expansion of fatigue wear mechanism, where repeated and constant sliding introduce dislocations in the sub-surface by plastic deformation, inducing cracks that eventually shear the surface and will form long thin wear sheets[69]. Figures 4-25 show cracks which are precursors of delamination, while in Figure 4-26 the formation of wear sheet is evident. Samples with higher amounts of diboride particles show that delamination is the dominant wear mechanism due to the formation of layers of debris attached to the surface (Figure 4-27). Depending on the rate of wear debris formation, delamination may result in a reduction of wear by the formation of a debris layer between the contacting surfaces (Figure 4-12)[24].

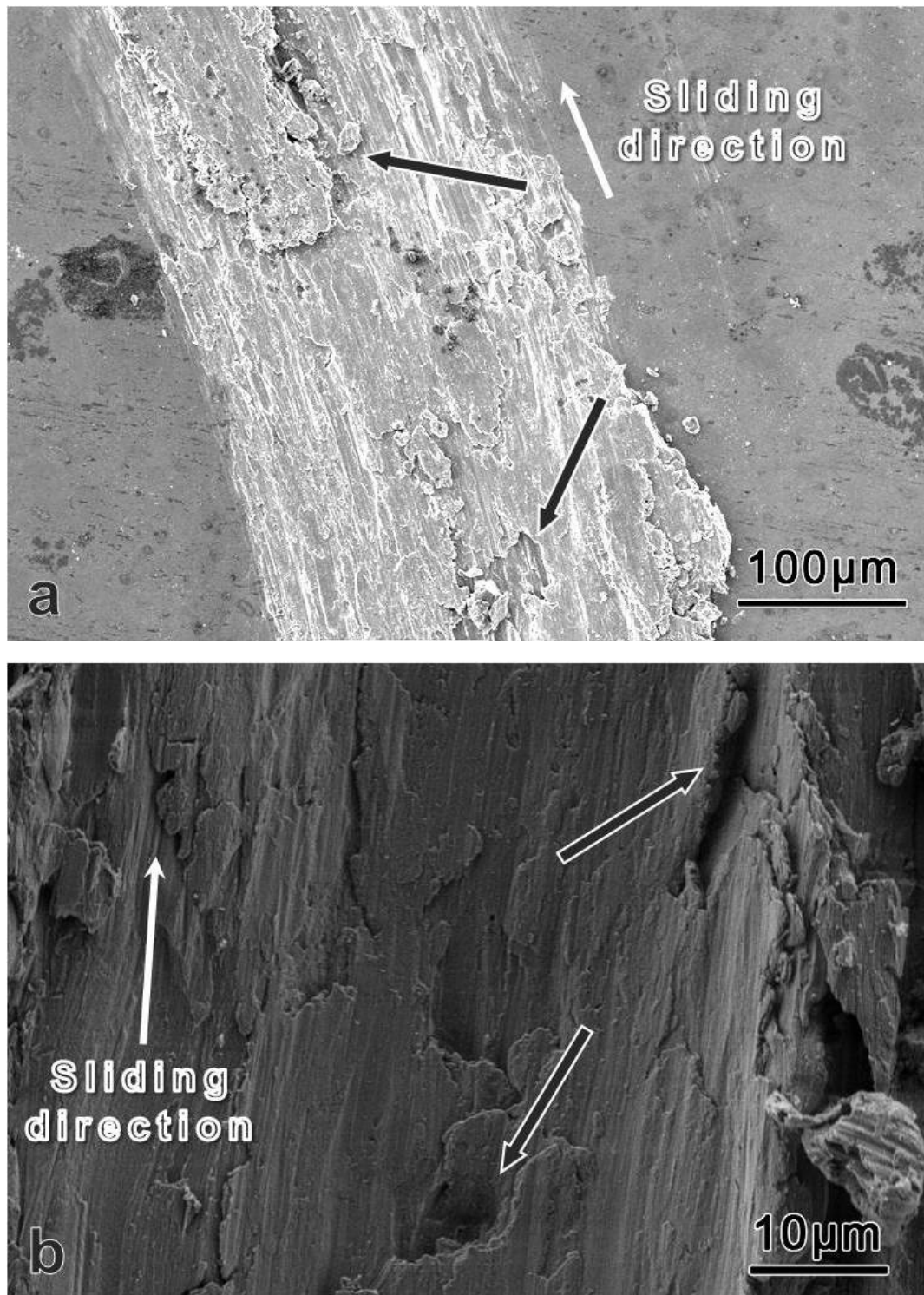


Figure 4-24: SEM micrographs showing evidence of delamination wear damage (arrows): a) Al-2.5%Cu-0%Mg-1%B composite, b) Al-2.5%Cu-1%Mg-3%B composite

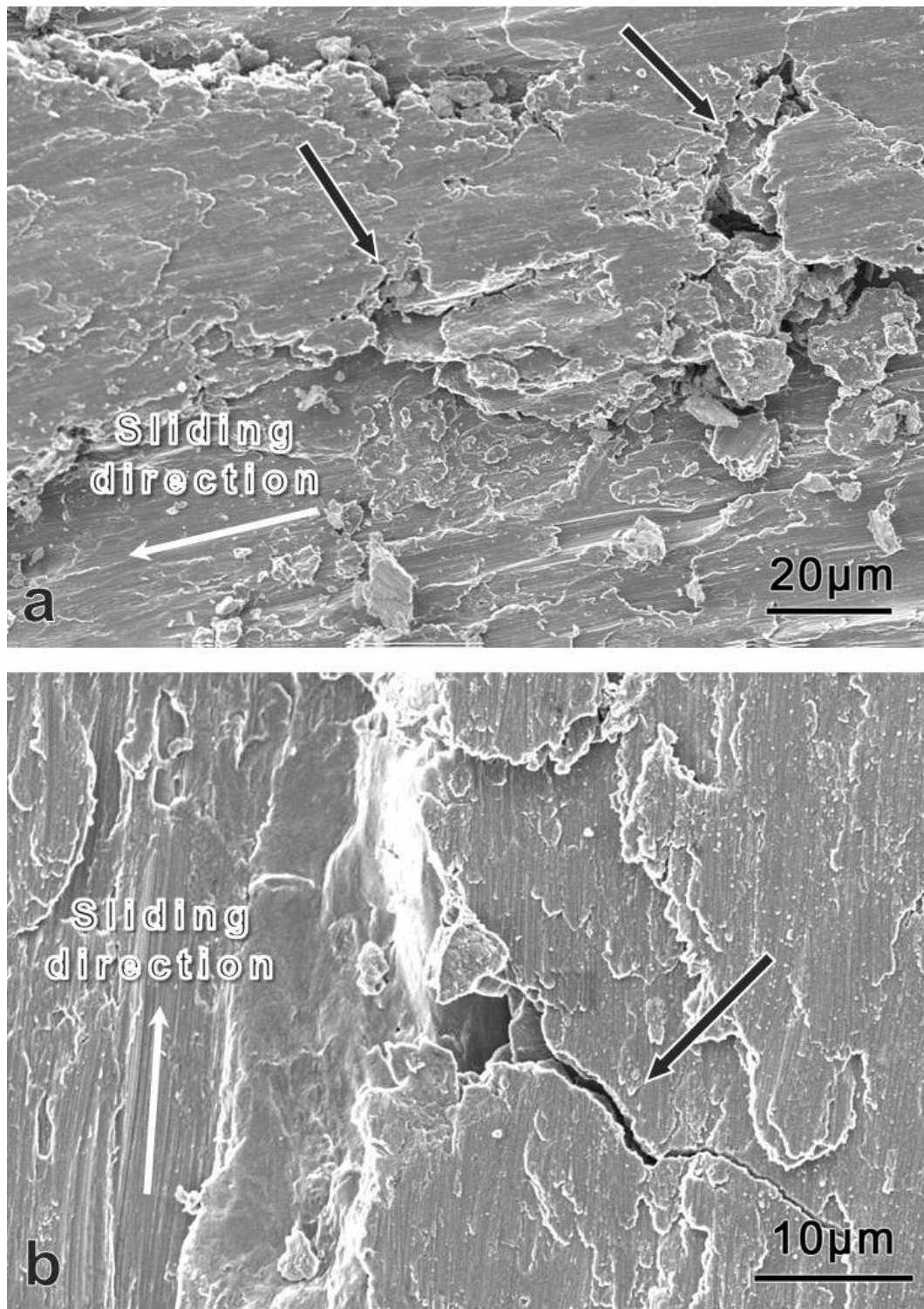


Figure 4-25: a)(arrows) Apparent delamination of Al-2.5%Cu-0%Mg-1%B composite and b)(arrows) prominent surface crack on Al-2.5%Cu-0%Mg-1%B composite

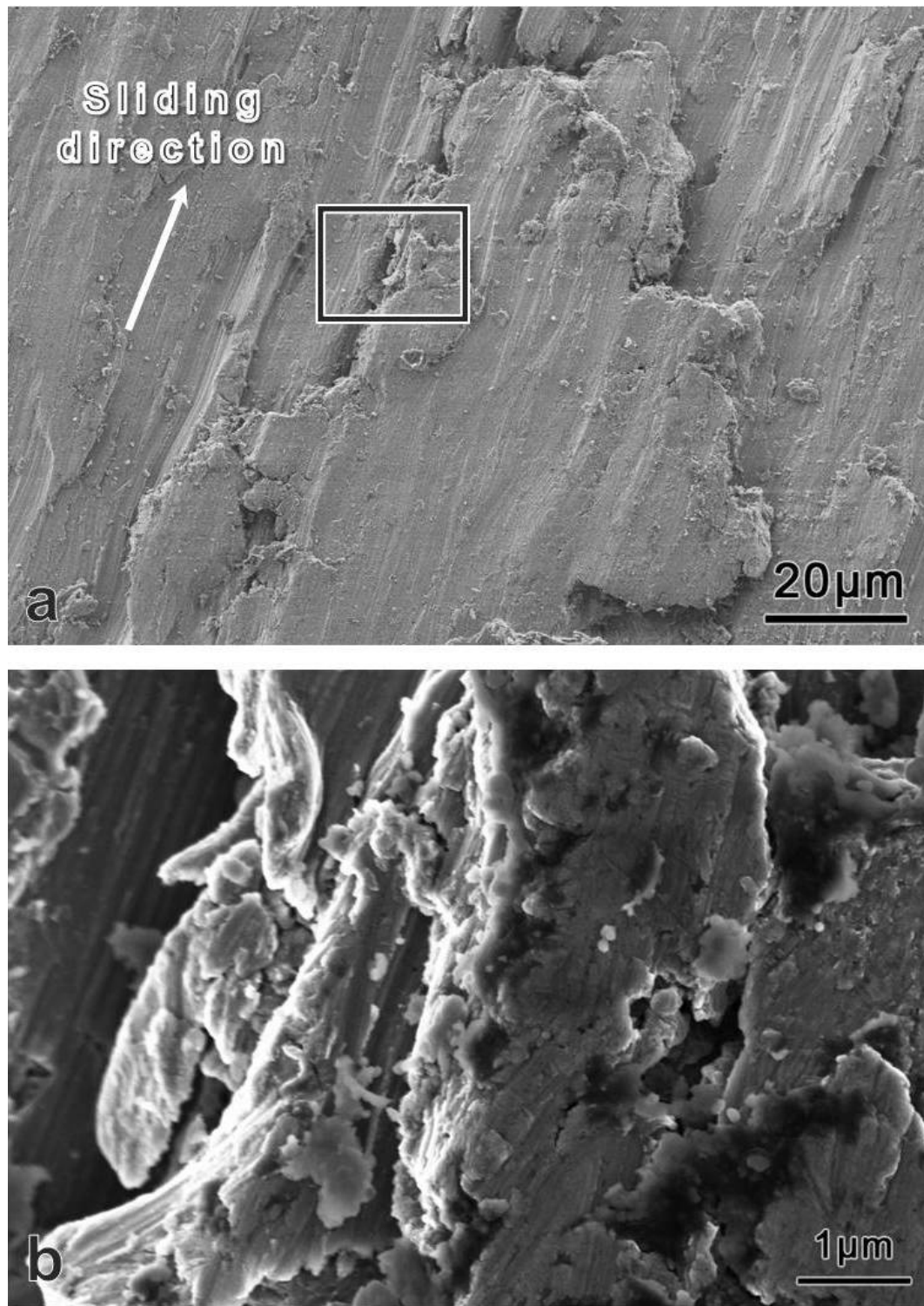


Figure 4-26: a)Wear sheet formation as observed using secondary electron imaging of Al-2.5%Cu-3%Mg-0%B composite b)rectangle in (a) at higher magnification

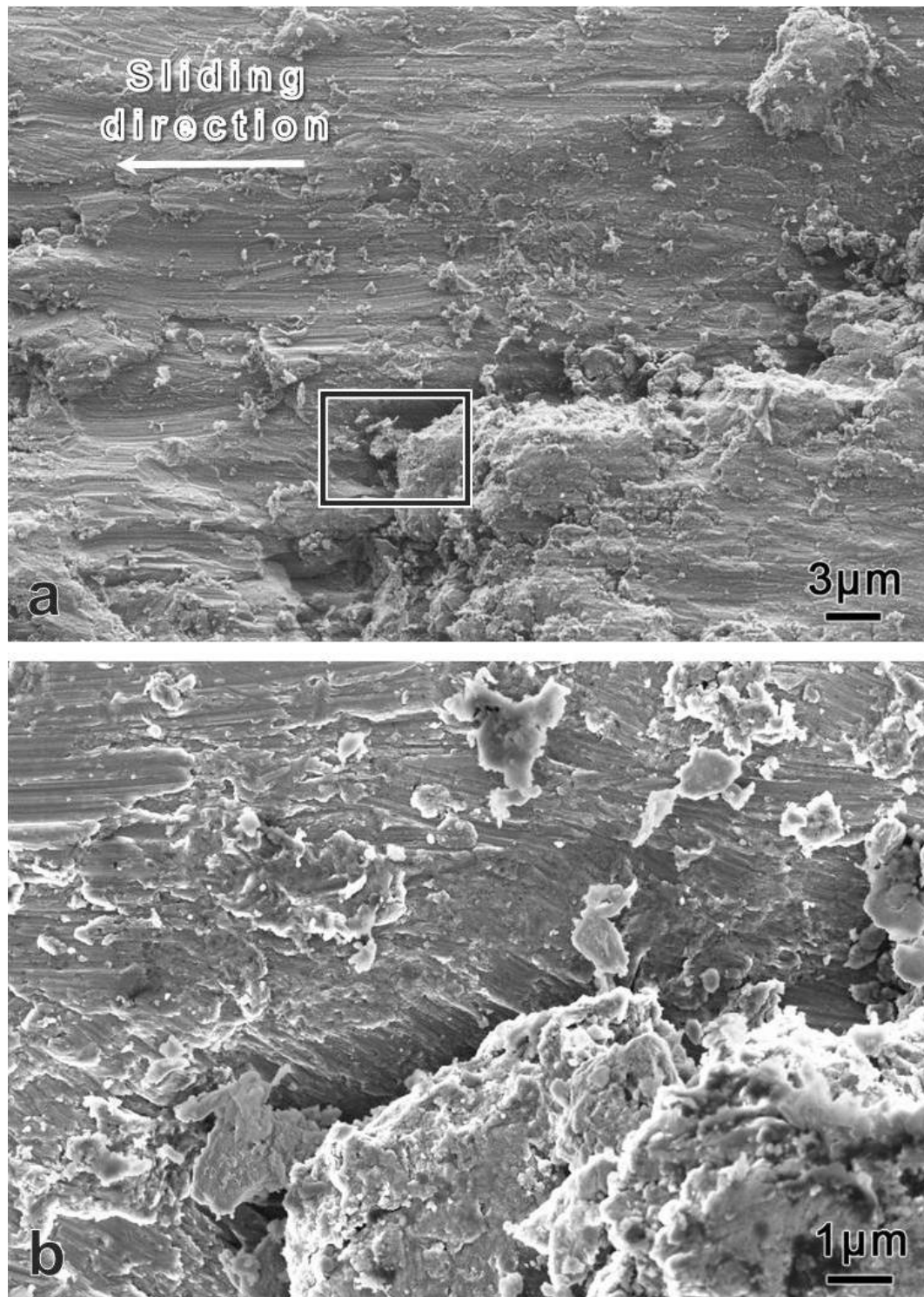


Figure 4-27: a) Layers of debris attached to the surface as a result of delamination wear in Al-2.5%Cu-3%Mg-3%B composite b) rectangle in (a) at higher magnification

4.4 Discussion

The results revealed a dependence of the wear resistance of the composites on the amount of reinforcement particles in the samples present. The composites with 0 wt.% to 2 wt.% of B are characterized by higher wear rates, which translate into lower wear resistance with respect to the composites with higher levels of boron. It is evident that the influence of AlB_2 particles reduce the wear volume and wear coefficient of the composites. These results are concurrent with the analysis made by Korkut[2] for the tribological behavior of aluminum matrix composites reinforced with particles. In agreement with this author, the trend of decreasing wear rate with increasing volume fraction of particles will be obtained because the particles remain well bonded with the matrix during sliding wear conditions, the aluminum matrix surrounding the particles will be worn away, and essentially all contact will be between the reinforcing particles and the steel counterface. This influence can be attributed to the supporting effect of the matrix to the diborides particles, enhanced by an appropriate interface bond[70]. Vencl et. al[71], also support this statement that softer metal matrix material is usually worn away first, leaving protrusions of the hard second phase of particles reinforcement which protect the metal matrix from further wear, the increase of particles volume fraction reduce the plastic deformation in the layer below the worn surface

as in Figure 4-27. Pruthviraj et. al[72] concluded that a soft matrix can secure the hard particles and improve the wear resistance of composite largely.

The results presented in this thesis clearly indicated that the reinforcement particles play a more direct role in the wear behavior of the composites rather than the hardness. Biswas[73, 74] stated that in tribology there is no necessarily direct correlation between wear resistance and hardness. Furthermore, Korkut[2] found that a decrease in wear rate of the composite cannot be correlated with higher hardness of the composite, since other parameters must be taken into account. The SEM observations and EDS analysis revealed that the diboride particles hide themselves under the worn surface[20] and the resistance to plastic flow become visible at places where clusters of AlB_2 are located as seen in Figure 4-28[75].

Additionally, as summarized in Table 4-3, the present work identified three wear modes affecting the worn surface of the composites: abrasive wear, oxidative wear and delamination wear. Despite the difference in the wear resistance and wear modes of the composites, in all cases plastic deformation occurred. The EDS analysis proved the absence of debris coming from the pin, i.e. stainless steel, since no adhered pin material was found on the wear track, as discovered in a previous research at UPRM [76]. Consequently, the adhesive wear

mechanism is not present and it can be assumed that the asperities on the pin remained in elastic contact with the surface of the composite. Examination of the wear tracks shows a change in the dominant wear mechanism present in the composite from abrasive wear to delamination wear when the level of boron is between 3 wt.% to 4wt.% as evidenced by the flake debris. Zhang and Alpas[77] examined cross-sections of worn surfaces of aluminum alloys reinforced with Sic particles, which showed evidence of wear debris in the form of flakes and supports the delamination theory. Even though for high levels of boron the dominant mechanism was found to be delamination wear, for these same samples the lowest wear rate was obtained. Analyzing these results, it is assumed that the delamination wear in conjunction with the oxidative wear mechanism are working as lubricants agents, maintaining a high wear resistance in the composites. Studies such as those of Chawla[24] and Zhang[78] suggest similar results with these wear mechanisms. Chawla stated that depending upon the rate of wear debris formation; delamination may result in a reduction of wear by the formation of a debris layer between the contacting surfaces. While Zhang proposed that oxidative wear mechanism is good for decreasing wear of the composites by means of the resulting oxidative particles or films that may produce a lubricating effect in the surface and reduce the wear.

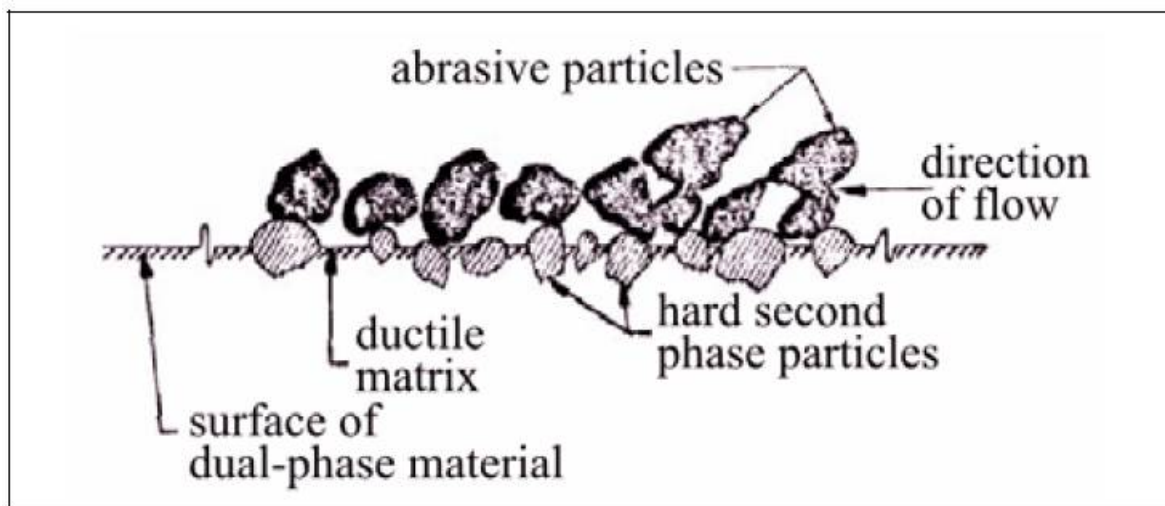


Figure 4–28: Schematic illustration of particles reinforcements protecting the matrix from wear

Table 4–3: Wear Mechanisms as function of boron percentage in the samples

Wear Mechanisms	Levels of Boron		
	Low	Medium	High
Abrasive	Dominant	Some	Scattered
Oxidative	Some	Some	Some
Delamination	Some	Scattered	Dominant

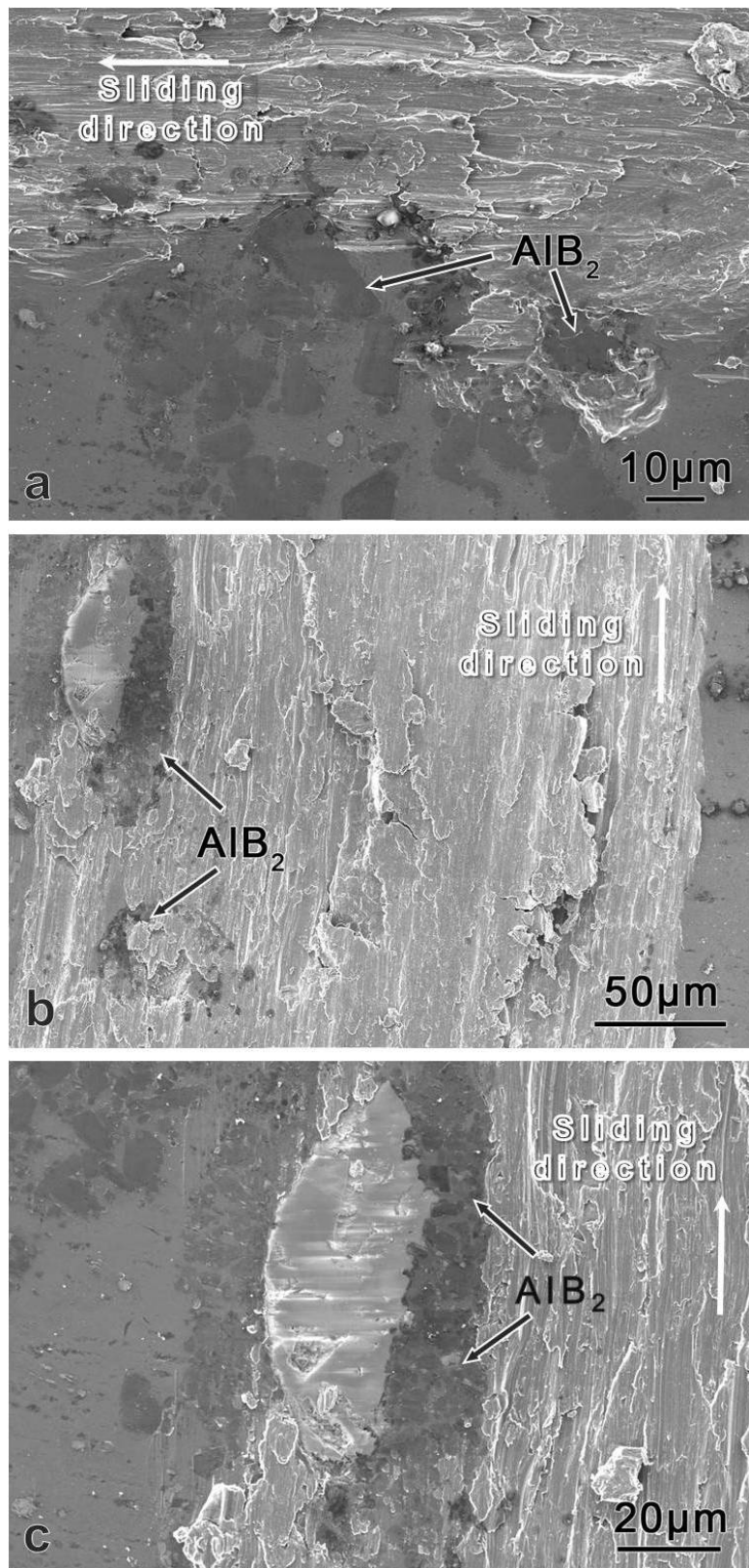


Figure 4-29: SEM images of: (a) and (b) show evidence of resistance to plastic flow of Al-2.5%Cu-0%Mg-1%B composite c)(b) at higher magnification

CHAPTER 5

CONCLUSIONS

The wear behavior of aluminum matrix composite containing copper and magnesium and reinforced with AlB_2 particles was investigated by pin-on-disk tests. Based on the obtained results, the following conclusions can be drawn:

- Samples containing 2.5 wt.%Cu, 1 wt.%Mg with varying boron levels revealed a decreasing tendency in the superficial hardness as the content of AlB_2 particles increased. It is inferred that such hardness drop is caused by an interaction between magnesium and the diboride particles, opening the opportunity of new research to understand the nature of such interaction.
- The wear volume and wear coefficient exhibit a general tendency to decrease influenced by the AlB_2 particles present in the composites. All composites exhibited similar behavior, i.e. as levels of boron increases, the wear volume and wear coefficient decreases.
- The lowest wear volume and wear coefficient was reached in Al-B-Cu-Mg composites containing 4 wt.% of boron.

- Three wear mechanisms were identified as responsible of the Al-B-Cu-Mg composites wear behavior under the test conditions: oxidative wear, abrasive wear and delamination wear.
- No transfer or adhered material from the pin to the surface worn was observed, thus no evidence of adhesive wear was found.
- A transition from abrasive to delamination wear takes place with the increase of diboride particles.
- Delamination wear and oxidative wear is assumed that work as lubricant agents to reduce wear on the composites with high levels of boron.
- The AlB_2 particles play a direct role in the wear behavior of the composite rather than the overall hardness. It can be concluded that the increment of boron levels in the composites affects the wear behavior of the composites, improving the wear resistance and making it a potential material for aerospace and automotive applications.

REFERENCE LIST

- [1] O.M. Suárez. Mechanical properties of a novel aluminum matrix composite containing boron. *J. of the Mechanical Behavior of Materials*, 12:225–237, 2001.
- [2] M.H. Korkut. Effect of particulate reinforcement on wear behaviour of aluminum matrix composites. *Materials Science and Technology*, 20:73–81, 2004.
- [3] P. Rohatgi. Metal matrix composite and method of producing. *Electric Power Research Institute, INC*, EP805726, 1997.
- [4] O.M. Suárez. Precipitation hardening of a novel aluminum matrix composite. *Materials Characterization*, 49:187–191, 2003.
- [5] O.M. Suárez; J. Yupa Luna; H. Calderón Arteaga. Precipitation hardening in novel aluminum matrix composite. *Transactions of the American Foundry Society*, 11:159–166, 2003.
- [6] E.G Totten. Physical metallurgy and process. *Handbook of Aluminium*, 1, 2003.
- [7] J. Actionb W.G. Sawyerb C.G. Toneyc R.W. Siegela L.S. Schadlera P. Bhimaraj, D.L. Burrish. Effect of matrix morphology on the wear and friction behavior of alumina nanoparticle/poly(ethylene) terephthalate composites. *Wear*, 258:1437–1443, 2005.
- [8] R.C. Rathod R.K. Paretkar S.G. Sapate, A. Uttarwar. Analyzing dry sliding wear behaviour of copper matrix composites reinforced with pre-coated sicp particles. *Materials and Design*, 30:376–386, 2009.
- [9] S. Ramanathan S. Anbu Selvan. Dry sliding wear behavior of as-cast ze41a magnesium alloy. *Materials and Design*, doi: 10.1016/j.matdes.2009.10.054, 2009.

- [10] K. Kawabata Y. Seki Y. Kawamura K. Kondoh, J. Umeda. Wear behavior of sintered magnesium matrix composites reinforced with mg_2si particle under wet sliding conditions. *Transactions of JWRI*, 37:45–50, 2008.
- [11] H.L. Sui Y. Wang C.L. Xu J.G. Wang K. Xiu, H.Y. Wang and Q.C. Jiang. The sliding wear behavior of ticp/az91 magnesium matrix composites. *Journal of Materials Science*, 41:7052–7058, 2006.
- [12] Y. Zhan and G. Zhang. Friction and wear behavior of copper matrix composites reinforced with sic and graphite particles. *Tribology Letters*, 17:91–98, 2004.
- [13] N.B. Dhokey and R.K. Paretkar. Study of wear mechanisms in copper-based sicp (20% by volume) reinforced composite. *Wear*, 265:117–133, 2008.
- [14] O. M. Suárez E. E. Hellstrom R.G.I. Hidalgo, S. Pedraza. Microcharacterization of al-b-cu composites. *TMS Letters*, 3:59–60, 2006.
- [15] Z.H. Melgarejo. Functionally graded aluminum matrix composites for high wear aerospace applications. *Master of Science Thesis, University of Puerto Rico-Mayagez*, 2006.
- [16] H.J. Rack A.P. Sannino. Dry sliding wear of discontinuously reinforced aluminum composites: review and discussion. *Wear*, 189:1–19, 1995.
- [17] J. Zhang A.T. Alpas. Wear rate transitions in cast alsi alloys reinforced with sic particles. *Scripta Metall. Mater*, 26:505–509, 1992.
- [18] P.K. Rohatgi M.K. Surappa, S.V. Prasad. Wear and abrasion of cast alalumina particle composites. *Wear*, 77:295–302, 1982.
- [19] M. Olsson S. Hogmark A. Alahelisten, F. Bergman. On the wear of aluminium and magnesium metal matrix composites. *Wear*, 165:221–226, 1993.
- [20] Y. Iwai T. Miyajima. Effects of reinforcements on sliding wear behavior of aluminum matrix composites. *Wear*, 255:606–616, 2003.
- [21] K. Sridharan Z.H. Melgarejo, O. M. Surez. Wear resistance of a functionally-graded aluminum matrix composite. *Scripta Materialia*, pages 95–98, 2006.

- [22] A.A. Aksenov N.A. Belov, D.G. Eskin. Multicomponent phase diagrams: applications for commercial aluminum alloys. *Elsevier Science, Amsterdam, The Netherlands*, page 87, 2005.
- [23] L.J. Yang. Wear coefficient equation for aluminum-based matrix composite against steel disc. *Wear*, 255:579–592, 2003.
- [24] K.K. Chawla N. Chawla. *Metal matrix composites*. Springer Science+Business Media; NY, 2006.
- [25] K.U. Kainer. *Metal matrix composites: custom-made materials for automotive and aerospace engineering*. Wiley-Vch; Weinheim, 2006.
- [26] J.R. Davis. *Aluminum and aluminum alloys ASM specialty handbook*. ASM International; OH, 5 edition, 1993.
- [27] M.K. Milauskas. *Metal matrix composites*. 2009 edition, <http://composites-by-design.com>.
- [28] M. Kozma. Friction and wear of aluminum matrix composites. *The Annals of University "Dunarea de Jos" of Galati Fascicle VIII, Tribology*, 34:99–106, 2003.
- [29] J. Liang K.C. Chan. Effect of microstructures on deformation behavior of aluminum matrix composites in laser bending. *Textures and Microstructures*, 34:43–54, 2000.
- [30] S. Rawal. Metal-matrix composites for space applications. *Journal of Alloys and Compounds*, 53:14–17, 2001.
- [31] A. Basumallick B. Basu D. Roy, S. Ghosh. Preparation of ti-aluminide reinforced in situ aluminium matrix composites by reactive hot pressing. *Journal of Alloys and Compounds*, 436:107–111, 2007.
- [32] *Composites material handbook: metal matrix composites*, volume 4. Department of Defense, 1999.

- [33] K. Ozdin Y. Sahin. A model for the abrasive wear behavior of aluminum based composites. *Materials and Design*, 29:728–733, 2008.
- [34] Y. Liu P.K. Rohatgi, S. Ray. Tribology of composite materials. *Conference Proceedings oakridge*, pages 1–14, 1990.
- [35] Chapter 2. *Aluminum matrix composites-processing and properties*. <http://cimewww.epfl.ch/people/cayron/Fichiers/thesebook-chap2.pdf>.
- [36] X. Wang. The formation of alb_2 in an al-b master alloy. *Journal of Alloys and Compounds*, 403:283–287, 2005.
- [37] J.E. Hatch. *Aluminum: properties and physical metallurgy*, volume 1. Aluminum Association, American Society for Metals, 1984.
- [38] H.K.D.H. Bhadeshia R. Cornell. *Metallographic specimen, aluminium-copper age hardening alloys*. <http://www.msm.cam.ac.uk/phasetrans/abstracts/M24.html>.
- [39] E.L. Rooy J.G. Kaufman. *Aluminum alloy castings: properties, processes, and applications*, volume 1. American Foundry Society, 2004.
- [40] R. Huang. *Aerospace materials laboratory*. <http://www.ae.utexas.edu/courses/ase324huang/Lecture6.pdf>, 2003.
- [41] L. Reyes. Synthesis and characterization of (almg) b_2 - aluminum based composites and nanocomposites. *Master of Science Thesis, University of Puerto Rico-Mayagez*, 2007.
- [42] B. Bhushan. *Introduction to tribology*. John Wiley and Sons, New York, 2002.
- [43] ASM Handbook. *Friction, lubrication, and wear technology*. ASM International, OH, 1992.
- [44] R. Chattopadhyay. *Surface wear: analysis, treatment, and prevention*. ASM International, OH, 2001.
- [45] D. Scott M.H. Jones. *Industrial tribology: the practical aspects of friction, lubrication and wear*, volume 1. Elseviers, 1983.

- [46] A. Ekberg. *Wear-some notes*. <http://www.am.chalmers.se/~anek/research/wear.pdf>, 1997.
- [47] Engineers Edge. *Adhesive wear*. <http://www.engineersedge.com/lubrication/adhesive-wear.htm>, 2000.
- [48] S.B. Kolla. Studies on corrosive wear mechanisms and models experimental set-up and studies on an austenitic stainless steel. *Master of Science Thesis, Indian Institute of Technology, Bombay*, 2002.
- [49] A.W. Batchelor G.W. Stachowiak. *Engineering tribology*. Butterworth Heinemann, 2001.
- [50] B. Bhushan. *Modern tribology handbook*, volume 1. CRC Press, 2001.
- [51] N.K. Myshkin M. Braunovic, V.V. Konchits. *Fundamentals of Electrical Contacts*. Taylor and Francis Group, CRC Press, 2007.
- [52] N.P.Suh. *Tribophysics*. Prentice-Hall, New Jersey, 1986.
- [53] R. Vilar R. Colaco. Abrasive wear of metallic matrix reinforced materials. *Wear*, 255:643–650, 2003.
- [54] B. Bhushan. *Principles and applications of tribology*. John Wiley, 1999.
- [55] J.F. Archard. Contact and rubbing of flat surfaces. *Journal of Applied Physics*, 24:24, 1953.
- [56] J.A. Williams J.J. Kauzlarich. Archard wear and component geometry. *Proc Instn Mech Engrs*, 215:387–403, 2001.
- [57] I.M. Hutchings. *Tribology: friction and wear of engineering materials*. Butterworth-Heinemann, 1992.
- [58] R.T. Maney N.J. Brown, P.C. Baker. Optical polishing on metals. *SPIE: Contemporary methods of optical fabrication*, 306:41–57, 1981.
- [59] A. Gessenharter E. Brinksmeier, O. Riemer . Finishing of structured surfaces by abrasive polishing. *Precision Engineering*, 30:325–336, 2006.

- [60] T. Kasai. A kinematic analysis of disk motion in a double sided polisher for chemical mechanical planarization (cmp). *Tribology International*, 41:111–118, 2008.
- [61] N. Neuroth H. Bach. *The properties of optical glass*, volume 2. Springer, New York, 1998.
- [62] H. Calderón. Efectos de la deformación mecánica sobre compuestos de matrix de aluminio tratados térmicamente. *Master of Science Thesis, University of Puerto Rico-Mayagez*, 2004.
- [63] T. Fujima A. Tanaka, S. Yoshimura and Ken ichi Takagi. Properties of boride-added powder metallurgy magnesium alloys. *Journal of Physics: Conference Series: 16th International Symposium on Boron, Borides and Related Materials*, 176, 2009.
- [64] H. Calderón. Effect of cycling high loading rates on fatigue behavior of al-based composites, chapter 4. *Ph. D. Dissertation, Civil Engineering, University of Puerto Rico-Mayagez*, 2009.
- [65] *Standard test method for wear testing with a pin-on-disk apparatus*. ASTM International, 2005.
- [66] *NewView 7000 series 3D optical surface profilers*. <http://www.zygo.com/?/met/profilers/newview7000/>.
- [67] H.A. Rothbart. *CAM design handbook*. McGraw Hill, 2004.
- [68] M. Gee M.J. Neale. *Guide to wear problems and testing for industry*. William Andrew, 2001.
- [69] E. P. Abrahamson N.P.Suh, S. Jahanuir. *The delamination theory of wear*. National Technical Information Service, US Department of Commerce, 1974.
- [70] D. Lu R. Zhou, Y. Jiang. The effect of volume fraction of wc particles on erosion resistance of wc reinforced iron matrix surface composites. *Wear*, 255:134–138, 2003.

- [71] I. Bobić A. Vencl, A. Rac. Tribological behaviour of al-based mmcs and their application in automotive industry. *Tribology in Industry*, 26, 2004.
- [72] P.V. Krupakara R.D. Pruthviraj. Friction and wear of al6061 containing 10wt.% sic metal matrix composites. *International Journal of Material Science*, 2:59–64, 2007.
- [73] S.K. Biswas. Wear of metals: a consequence of stable/unstable material response. *Proc Instn Mech Engrs Part J: J Engineering Tribology*, 216:357–369, 2002.
- [74] S.K. Biswas. *New directions in tribology*. Mechanical Engineering Publications, London, 1997.
- [75] S. Das. Development of aluminum alloy composites for engineering applications. *Trans. Indian Inst. Met.*, 57:325–334, 2004.
- [76] K. Sridharan Z.H. Melgarejo, O.M. Surez. Microstructure and properties of functionally graded almgc composites fabricated by centrifugal casting. *Composites: Part A*, 39:1150–1158, 2008.
- [77] A.T. Alpas J. Zhang. Delamination wear in ductile materials containing second phase particles. *Materials Science and Engineering Part A*, 160:25–35, 1993.
- [78] Y.W. Mai Z.F. Zhang, L.C. Zhang. Wear of ceramic particle-reinforced metal-matrix composites. *Journal of Materials Science*, 30:1961–1966, 1995.